Unlocking archival maps of the Hornsund fjord area for monitoring glaciers of the Sørkapp Land peninsula, Svalbard

Justyna Dudek[1] **and Michał Pętlicki**[2,3]

[1]Institute of Geography and Spatial Organization Polish Academy of Sciences (IGSO PAS), Warsaw, Poland
[2]Faculty of Geography and Geology, Jagiellonian University, Kraków, Poland
[3]Department of Geography, Universidad de Concepción, Concepción, Chile

Correspondence: Justyna Dudek (justyna_dudek@wp.pl)

Abstract. Archival maps are an important source of information on the state of glaciers in polar zones and are very often basic research data for analysing changes in glacier mass, extent, and geometry. However, basing a quantitative analysis on archival maps requires that they be standardised and precisely matched against modern-day cartographic materials. This can be achieved effectively using techniques and tools from the field of geographic information systems (i.e. GIS). The objective of this research was to accurately register archival topographic maps of the area surrounding the Hornsund fjord (southern Spitsbergen) published by the Polish Academy of Sciences and to evaluate their potential for use in studying changes in the geometry of glaciers in the north-western part of the Sørkapp Land peninsula in the following periods: 1961–1990, 1990–2010, and 1961–2010. The area occupied by the investigated glaciers in the north-western Sørkapp Land decreased in the years 1961–2010 by $45.6\,\mathrm{km}^2$, i.e. by slightly over 16 %. The rate of glacier area change varied over time and amounted to $0.85\,\mathrm{km}^2\,\mathrm{yr}^{-1}$ in the period 1961–1990 and sped up to $1.05\,\mathrm{km}^2\,\mathrm{yr}^{-1}$ after 1990. This process was accompanied by glacier surface lowering by about 90–100 m for the largest land-terminating glaciers on the peninsula and by up to more than 120 m for tidewater glaciers (above the line marking their 1984 extents). The dataset is now available from the Zenodo web portal: https://doi.org/10.5281/zenodo.4573129 (Dudek and Pętlicki, 2021).

1 Introduction

The Svalbard archipelago (Fig. 1a and b) is among the regions that have experienced the fastest climate warming recorded in the Arctic after the Little Ice Age (LIA) (Nordli et al., 2020). Since the beginning of the last century, the average annual temperature in this area has increased by $2.6\,°\mathrm{C}$ per century, which is more than twice the average for other areas of the world (Nordli et al., 2014). In addition, a rapid acceleration of the pace of this process has been observed since the late 1990s (Isaksen et al., 2016). The current intensification of climate change translates to the evolution and dynamics of glacier systems, resulting in their negative mass balance and frontal recession (Nuth et al., 2010; Morris et

al., 2020; Schuler et al., 2020). Changes in glacier geometry constitute a visible and easily measured parameter that, in addition to being a reliable indicator of its condition, is a proxy of changes in the natural environment (Knight, 2006).

Glaciers on Svalbard have received less attention in past research than those in continental Europe (WGMS, 2020). This is due to their inaccessibility, harsh climatic conditions, and long polar nights, which limit the possibilities for direct measurement. Logistic and economic aspects play a crucial role in the selection of research areas, so data collection to document glacier changes (including field measurements) focuses mainly on the more accessible western coasts of the Spitsbergen island (Hagen and Liestøl, 1990). The use of traditional research methods, e.g. in situ stake mass balance
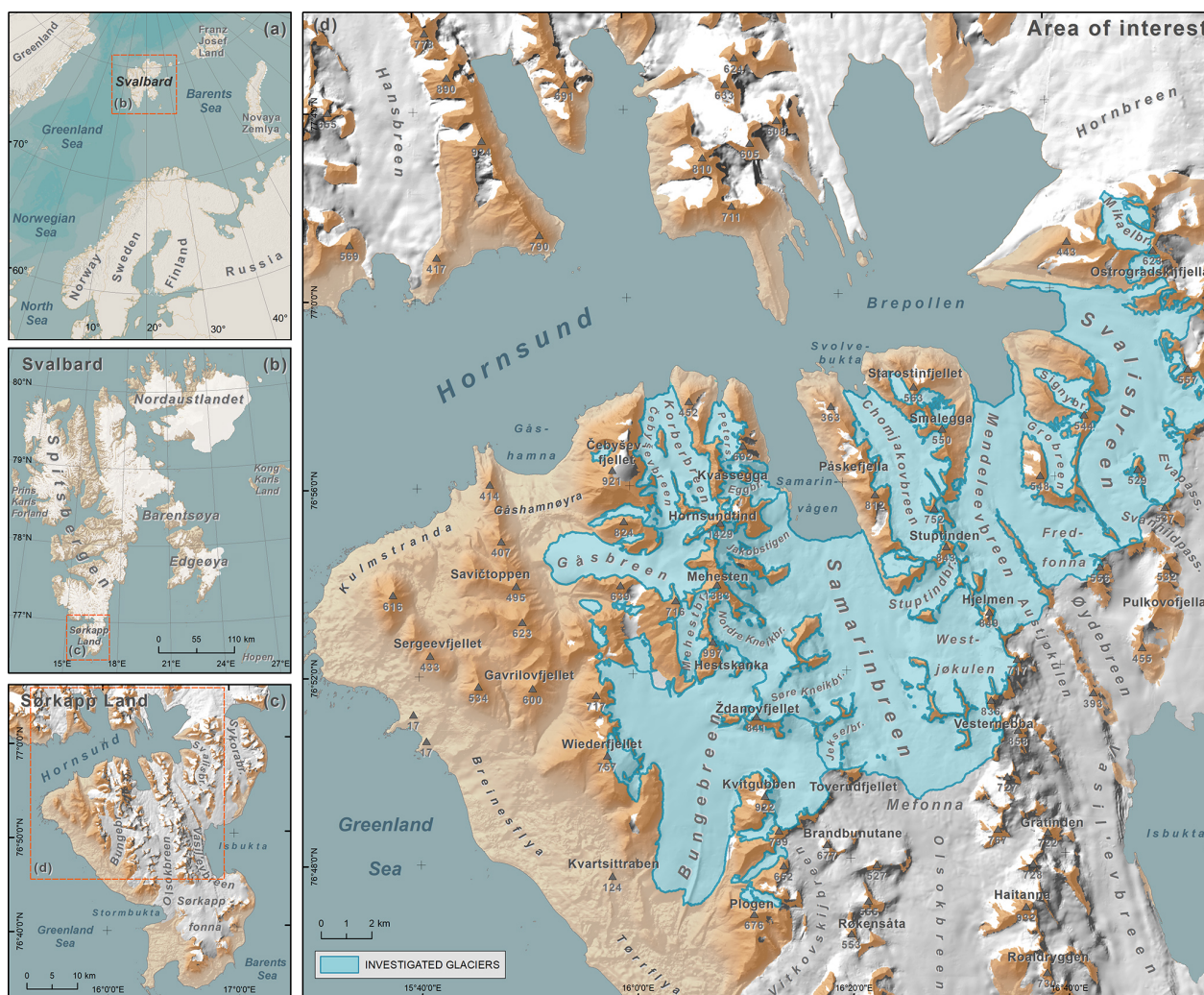
Figure 1. Location of the study area in the background of **(a)** the Svalbard archipelago, **(b)** the Sørkapp Land peninsula, and **(c)** its north-western part. Background maps based on NPI (2014).

measurements, is costly and time-consuming, even if the research programme is reduced to a minimum, so changes in the geometry of Svalbard glaciers are often inferred from satellite data and aerial photographs (Jacob et al., 2012; Nuth et al., 2013; Martín-Moreno et al., 2017; Girod et al., 2018; Geyman et al., 2022). The use of remote sensing has a number of advantages in glacier research, the most important of which is that the data do not require a large team in the field and can be used to quickly generate precise results. These factors have certainly contributed to the use of remote sensing methods since almost the very beginning of glaciological research (Finsterwalder, 1954; Stocker-Waldhuber et al., 2019; Mannerfelt et al., 2022).

In the initial period of polar research based on remote-sensing methods, ground-based photogrammetry techniques were mainly used. In Svalbard, terrestrial photogrammetric methods were first used in 1898 as part of topographic work

carried out by a Swedish expedition led by A. G. Nathorst (Nathorst, 1909). Later, these techniques were successfully used on several research expeditions organised, among others, by the prince of Monaco in 1906 and 1907 (Isachsen et al., 1912–1914), as well as on numerous Norwegian expeditions in 1909–1926 (Hoel, 1929). The aim and scientific fruit of the first photogrammetric work on Svalbard were, above all, topographic maps of poorly known areas, which were also valuable material for the study of glacier extents. Polish achievements in this field include a series of photogrammetric images and triangulation measurements made in 1934 as part of the first Polish research expedition to the as-yet-unexplored Torell Land (southern Spitsbergen), which yielded the first map of this area at a scale of 1 : 50 000 (Zagrajski and Zawadzki, 1936).

The construction of the Polish Polar Station on Isbjørn-hamna bay in 1957 allowed scientific teams to operate in

southern Spitsbergen. In the first years of the station, a Polish research team, led by C. Lipert, conducted terrestrial photogrammetric measurements, resulting in the production of detailed maps of glaciers in the vicinity of the Hornsund fjord (Kosiba, 1960; Lipert, 1962). Additionally, topographic sketches of the Antoniabreen and Penckbreen glaciers were made during an expedition to the vicinity of Van Keulenfjorden in the same period (Marcinkiewicz, 1961). Changes in the extent of glaciers around the station were also documented in the early 1970s, when summer expeditions of the University of Wrocław were held there (Żyszkowski, 1982), and, after activity resumed in 1978, on numerous expeditions carried out mainly by the University of Silesia and the Institute of Geophysics of the Polish Academy of Sciences (Instytut Geofizyki, Polska Akademia Nauk, hereinafter referred to as IGF PAN) (Kolondra, 2000). Terrestrial photogrammetric methods are still used today in glaciological studies of this area, and the longest series of measurements have covered the Werenskioldbreen, Torellbreen, and Hansbreen glaciers (Kolondra, 2002).

Compared to other areas of Svalbard, the photogrammetric research on the Sørkapp Land peninsula and the number of related cartographic work published are very modest. The area most often chosen for cartographic studies has been the north of the peninsula (which is relatively accessible from the Hornsund fjord), including mainly the Gåsbreen area (De Geer, 1923; Pillewizer, 1939; Jania, 1979, 1982; Kolondra, 1979, 1980; Schöner and Schöner, 1996, 1997; Ziaja et al., 2016) and the glaciers that flow into the fjord (Heintz, 1953; Błaszczyk et al., 2013).

Terrestrial photogrammetric methods provide precise and repeatable results. However, they can only be used for small-scale studies, usually covering one glacier or its foreland (Kolondra, 2005). For glaciological studies with extensive spatial coverage, data obtained from the aerial ceiling are much more competitive, providing information from large and hard-to-reach areas, which is of great importance in polar conditions. Therefore, aerial photogrammetry progressed along with ground measurement techniques on Svalbard. Professional photogrammetric overflights by the Norwegian Polar Institute (NPI) covered the entire or almost all of the Sørkapp Land peninsula (Table 1). The first, in 1936, resulted in a series of oblique photos that were used to create a 1 : 100 000 topographic map that covered the entire Svalbard archipelago (Luncke, 1936; NPI, 1986; Geyman et al., 2022). Another map by the Norwegian Polar Institute was published only in 2007, and it was based on 1 : 50 000 vertical photos from 1990, this time as colour prints (NPI, 2007). For the study of glacier evolution and glacial landforms on the Sørkapp Land peninsula, the series of photos taken in 1961 is of great importance, because, for the first time in the history of this area, it uniformly covered all its glaciers along with their marginal zones. Another dataset of the same spatial extent had not been created until 2010 (Fig. 2).
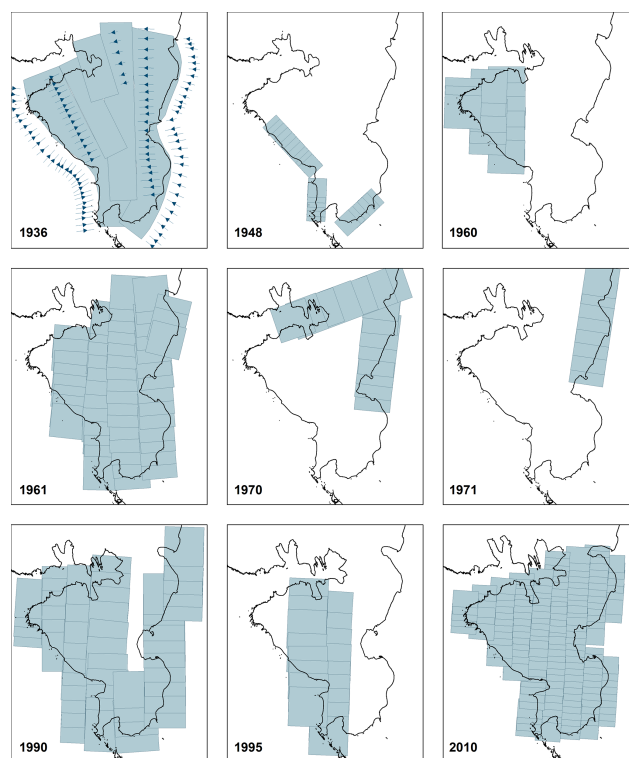

Figure 2. Norwegian Polar Institute photogrammetric campaigns carried out over the Sørkapp Land peninsula.

Norwegian photos from two photogrammetric campaigns in 1960 and 1961 have served as the source material for many cartographic and glaciological studies: Klysz and Lindner (1982); Ostaficzuk et al. (1982); Jania (1987, 1988a, b); Schöner and Schöner (1996); James et al. (2012); Błaszczyk et al. (2013); and Małecki (2013). Of the available cartographic studies valid for 1960/61, the 1 : 25 000 topographic map of the Hornsund fjord area has the greatest spatial coverage (1600 km^2). The series of sheets published in 1987 was, in part, the result of the IGF PAN programme of expeditions to Spitsbergen in the years 1979–1984 with the support of officers of the Polish military cartographic institute (Wojskowe Zakłady Kartograficzne) in conducting desk research and field work. Field survey reference photogrammetric measurements were made during the sixth expedition of the Polish Academy of Sciences in 1984. The present study aims to assess its accuracy and its potential for use in research on changes in glacier geometry on the north-western Sørkapp Land peninsula.

The use of archival cartographic data is one of the key ways to quantify mainly climate-change-related changes in the cryosphere (Nuth et al., 2007, 2013; Surazakov et al., 2006; Weber et al., 2020; Holmlund, 2021). On a global scale, such data on the topography of glaciers from the 1960s are relatively scarce – they are mainly based on a few photogrammetric surveys and the resultant topographic maps

Table 1. Norwegian Polar Institute photogrammetric campaigns carried out over the Sørkapp Land peninsula.

Year	Area of Sørkapp Land covered	References
1936	Entire peninsula	Błaszczyk et al. (2013), Dowdeswell et al. (1995), Geyman et al. (2022), Hagen et al. (1993), Heintz (1953), Jania (1988a, b), Jiskoot et al. (2000), König et al. (2014), Lefauconnier and Hagen (1991), Luncke (1936), Martín-Moreno et al. (2017), Noormets et al. (2020), NPI (1948, 1986, 2014), Nuth et al. (2007, 2013), Pälli et al. (2003), Sharov (2006), Sharov and Osokin (2006), Sund et al. (2009), Szafraniec (2018, 2020), Ziaja (2001, 2004), Ziaja et al. (2007, 2009), Ziaja and Ostafin (2015)
1948	Western and southern coasts	–
1960	Western part of the peninsula	Błaszczyk et al. (2013), Hagen et al. (1993), Jania (1987, 1988a, b), Schöner and Schöner (1996, 1997), Ziaja (2004)
1961	Almost entire peninsula except the NW	Barna and Warchoł (1987), Grabiec et al. (2017), Jania (1987, 1988a, b), Jania and Szczypek (1987), Klysz and Lindner (1982), Lefauconnier and Hagen (1991), Noormets et al. (2020), Ostaficzuk et al. (1982), Schuler et al. (2020), van Pelt et al. (2019, 2021), Ziaja (2004), Ziaja et al. (2007, 2016)
1970	Isthmus and eastern coast	Dowdeswell et al. (1995), Lefauconnier and Hagen (1991), Noormets et al. (2020), Nuth et al. (2013), NPI (2014), Schuler et al. (2020), van Pelt et al. (2019, 2021), Ziaja (2004)
1971	Eastern coast	Dowdeswell et al. (1995), Lefauconnier and Hagen (1991), Ziaja (2004), Ziaja et al. (2007, 2009)
1990	Almost entire peninsula except the NE	Błaszczyk et al. (2013), Fürst et al. (2018), Jiskoot et al. (2000), König et al. (2014), Noël et al. (2020), NPI (2014), Nuth et al. (2007, 2010, 2013), Schöner and Schöner (1996, 1997), Schuler et al. (2020), Sund et al. (2009), Szafraniec (2020), van Pelt et al. (2019, 2021), Ziaja (2004), Ziaja et al. (2007, 2016), Ziaja and Dudek (2011), Ziaja and Ostafin (2015)
1995	Central part of the peninsula	NPI (2014)
2010	Entire peninsula	Farnsworth et al. (2016), Fürst et al. (2018), NPI (2014), Ziaja et al. (2016)

(Tielidze, 2016; Andreassen et al., 2020) as well as a re-analysis of declassified spy satellite images (Bhambri et al., 2011; Bhattacharya et al., 2021; Maurer et al., 2015, 2019). In the Spitsbergen region, 1930s surveys are a key reference point for observed changes in area and volume (Nuth et al., 2007). Structure-from-motion (SfM) photogrammetry allows for better and more precise use of these photos and the creation of more accurate elevation models (Mertes et al., 2017; Midgley and Tonkin, 2017; Girod et al., 2018; Holmlund, 2021; Geyman et al., 2022). Unfortunately, high-quality scans of aerial imagery from 1961 that could be used to generate new DEMs using stereophotogrammetry or structure-from-motion methods were not available for this study. An attempt was made to process low-resolution scans with Agisoft Photoscan; however, the results were not satisfactory. The primary focus of the study was on the use and recovery of historical maps.

2 Study area

The Svalbard archipelago is surrounded by the Greenland Sea to the west, the Barents Sea to the east, and the Arctic Ocean to the north. The temperature of the bordering water masses influences its climate, which is milder than that of other areas at similar latitudes and, at the same time, more sensitive to changes related to the passage of atmospheric fronts (Hagen et al., 1993; Eckerstorfer and Christiansen, 2011). The East Spitsbergen Current transports cold Arctic waters along the eastern shores of the archipelago, whereas the West Spitsbergen Current, a branch of the Gulf Stream, brings warm Atlantic waters to the western shores. The resulting strong climate gradients cause a pronounced latitudinal and longitudinal variability in the ice cover of Svalbard, with the central part of Spitsbergen being largely ice free due to low precipitation and with the eastern shores being more glaciated than the western. Many of the Svalbard glaciers have surged in the recent past (Farnsworth et al., 2016) or are currently undergoing an active surge phase (Sund et al., 2009), with a substantial short-term increase in ice

flow velocity. Sørkapp Land is the southernmost peninsula of Spitsbergen, the largest island of the Svalbard archipelago (Fig. 1a and b). It is separated from the rest of Spitsbergen by the Hornsund fjord and a narrow glaciated isthmus of Hornbreen–Hambergbreen (Ziaja and Ostafin, 2015). There is ongoing speculation on whether Sørkapp Land will form a separate island when the ice in the isthmus is gone (Pälli et al., 2003; Grabiec et al., 2017). Compared to the rest of Svalbard, Hornsund and Sørkapp Land have a mild and humid climate (Isaksen et al., 2016). Meteorological measurements were not carried out until the 1970s in southern Spitsbergen. According to Førland et al. (2011), the mean annual temperature at Svalbard Airport in the period of 1966–1988 increased by 0.52 °C per decade, and in the following period (1988–2011) this trend continued with an increase of the mean annual temperature to 1.25 °C per decade. In recent decades, a similar trend was observed in southern Spitsbergen, where a pronounced increase in winter air temperature and summer precipitation sums was observed at the Polish Polar Station, Hornsund, where, in the period 1971–2000, the mean annual temperature was −4.7 °C which in the following years (2001–2015) increased by 1.9 °C (Førland et al., 2011; Osuch and Wawrzyniak, 2017).

The north-western Sørkapp Land region extends between the open Greenland Sea and the Hornsund fjord (Fig. 1c and d). It hosts 20 land-terminating glaciers, 8 tidewater glaciers, several rock glaciers, and numerous glacierets and perennial snow patches. The largest land-terminating glaciers in the analysed area are Gåsbreen, which is surrounded by the highest mountain massifs of southern Spitsbergen and fed by the Bastionbreen and Garwoodbren tributary glaciers, both of which rest on the slopes of the Hornsundtind massif; and Bungebreen, which extends meridionally between the high Hestskanka massif to the north and the Tørrflya coastal lowland to the south. The two largest glacial systems in western Sørkapp Land are surrounded by smaller valley and cirque glaciers. East of Samarinvågen bay, there are also several smaller land-terminating glaciers that constitute former tributaries of larger glaciers flowing into the Hornsund fjord.

Of the 16 glaciers flowing into the Hornsund fjord, 8 are located in the study area. These glaciers have a northern exposure, and their snouts move northwards. Some of them originate on glaciated mountain passes in the interior of the peninsula where they share their accumulation zones with other glaciers. Samarinbreen, which flows into Samarinvågen, one of the bays in the Hornsund fjord, is the largest tidewater glacier in the region. It flows from the Mefonna ice plateau, where it connects to the Olsokbreen glacial system that flows into the Greenland Sea. To the east, Samarinbreen is adjacent to the glaciers feeding the Vasil'evbreen glacier basin and to the west to the wide accumulation zone of Bungebreen. Samarinbreen is a compound glacier basin fed by numerous tributary glaciers, e.g. Westjøkulen and Stuptindbren, flowing westward from the slopes of Vesternebba, Hjelmen, and Stuptinden; and eastward-

flowing tributaries, e.g. Jekselbreen, Søre Kneikbreen, Nordre Kneikbreen, and Jakobstigen, situated in depressions between the Toverudfjellet and Hornsundtind massifs.

Further east of Samarinbreen are the Mendeleevbreen and Svalisbreen that flow into Brepollen bay. Both glaciers have a broad connection to the adjacent basin of Vasil'evbreen. Mendeleevbreen flows from the Austjøkulen ice plateau, and it receives additional supply from the Fredfonna ice plateau and Grobreen. The neighbouring Svalisbren occupies a depression with an atypical sinusoidal course. The main accumulation zone of the glacier is located on the Svanhildpasset.

In the depression between the Påskefjella and Smalegga massifs, there is the fourth largest glacier in the region – Chomjakovbreen, which fills a separate valley and does not connect with other glaciers. It calves with a not very wide cliff to the small Svovelbukta bay. It is fed by small but very numerous tributary glaciers located in cirques on the slopes of the surrounding mountain massifs. The longest tributary that feeds it is Dmitrievbreen.

In addition to the vast compound glacier basins, a number of smaller valley glaciers also flow into the Hornsund fjord. These include Körberbreen, with the Čebyševbreen tributary, and Petersbreen, Kvasseggbreen, and Eggbreen glaciers, which are to the west of Samarinbreen, where they fill deep valleys. They are distinguished from other outlet glaciers by their significant vertical range and associated steeper surface, which is due to the fact that their basin boundaries run along the highest mountain ranges of southern Spitsbergen: Čebyševfjellet (914 m a.s.l.), Vesletinden (928 m a.s.l.), Hornsundtind (1429 m a.s.l.), and Kvassegga (1004 m a.s.l.) (Jania, 1987). Körberbreen and Petersbreen lie in separate longitudinal mountain valleys whose depth and direction are determined by the geological structure of the substrate, which relates to the course of faults. The two small glaciers Kvasseggbreen and Eggbreen, which run adjacent to them to the east, run latitudinally and flow into Samarinvågen bay. They formerly served as the tributary glaciers to Samarinbreen, but as its snout has receded, they split from it and today constitute separate calving glaciers.

3 Source material

The basis for the spatial analysis consisted primarily of topographic maps and DEMs, supplemented with aerial photos and satellite images. A specification of these datasets is provided below.

3.1 Maps

3.1.1 IGF PAN topographic map series

The IGF PAN topographic map series, made in a Universal Transverse Mercator (UTM) projection (Northern Hemisphere, zone 33) based on a European Datum 1950 (ED50) ellipsoid, consists of 10 sheets. This study assessed six of
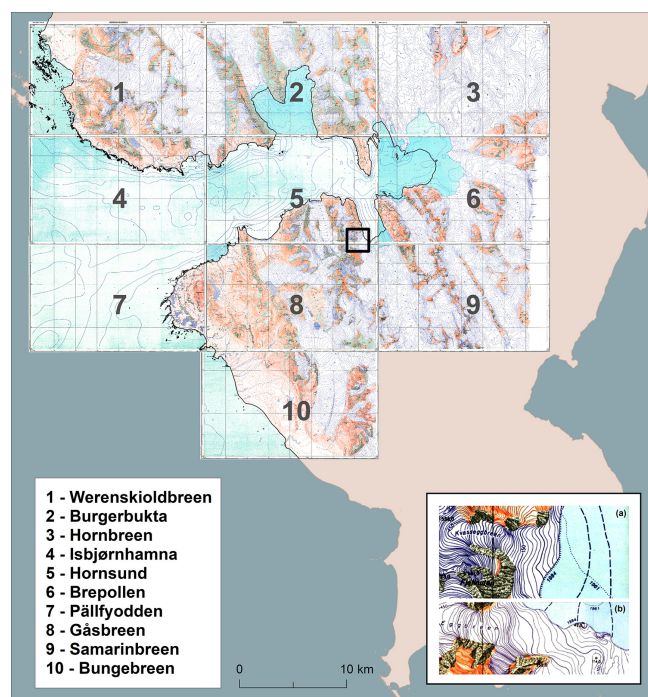
Figure 3. IGF PAN topographic map series published in 1987 (Barna and Warchoł, 1987). Example visualisations of the extents of tidewater glaciers on IGF PAN maps published in 1987: **(a)** Kvasseggbreen (Sheet 5 – Hornsund); **(b)** Eggbreen (Sheet 8 – Gåsbreen).

those sheets that represented glaciers with adjacent marginal zones and one sheet representing ice-free area in the territory of Sørkapp Land peninsula (no. 3: Hornbreen, no. 5: Hornsund, no. 6: Brepollen, no.7: Pällfyodden, no. 8: Gåsbreen, no. 9: Samarinbreen, and no. 10: Bungebreen; Fig. 3).

The topographic map sheets presented the relief, permanent and periodic watercourses, waterbodies, wetlands, glaciers, triangulation and topographic points, vegetation types (tundra), marine coasts (skerries), and names of geographical features (Fig. 3). The relief is presented using contour lines with contour intervals of 5 m for the relatively flat coastal plains and 10 m for steeper areas. Areas too steep to be mapped using contour lines in the assumed scale were presented as rock cliff symbols. The extents of land-terminating glaciers are marked as a change in contour line colour from orange (land) to blue (glacier), but lines were not drawn to mark the maximum extent of glacial snouts. Two extents are marked for tidewater glaciers (Petersbreen, Kvasseggbreen, Eggbreen, Samarinbreen, Chomjakovbreen, Mendeleevbreen, and Svalisbreen). The first – a dotted line on the surface of the Hornsund fjord – showed the position of their termini in 1961. The second extent, represented as ice cliffs, was the 1984 update of their boundaries (Fig. 3a and b).

When individual sheets were converted to digital form, it was important to take into account the particularity of the maps that resulted from the means by which they were created. Initial photogrammetric sketches of individual sheets were made using the 1961 Norwegian aerial photos from before the expeditions to Spitsbergen of the early 1980s (including the expedition to Sørkapp Land in the summer of 1984; Wiesław Ziaja, personal communication, 2011). The cartographic material constituted a base that, according to the information provided in the map description, was "partially checked and supplemented in the field".

Information on the degree to which documentation of the extent and elevation of Sørkapp Land glaciers was updated in the field was key in assessing the potential of this series for use in analysing changes in glacier thicknesses in the periods 1961–1990–2010. In the context of this analysis, the most important question was whether the contour lines marking the elevation of the glaciers represent the year 1961 (which would result from the use of aerial photographs from that period) or 1984 (which would result from the contour lines having been updated using field measurements made more than two decades after the photogrammetric overflight). The comparison of the 1987 series of maps with other cartographic studies of the area presenting the state of glaciers in the early 1960s led to the unequivocal conclusion that the contours contained therein represent the year 1961 (and thus were not corrected based on field research), while their updating (by "in-field supplementation") to reflect the 1984 state of affairs related only to glacier extents, as reflected in the change in contour colours.

One such study was a report from an expedition by Austrian scientists Monika and Wolfgang Schöner, who in 1991 made ground-based photogrammetric measurements on the forefield of Gåsbreen. These studies were based on photos from NPI's photogrammetric overflight over the west of Sørkapp Land in the summer of 1960 (Table 1) and resulted in a publication that included a map showing the hypsometric variation of Gåsbreen and a hillshade that was valid for 1960 (Schöner and Schöner, 1996). A helpful publication for comparisons of the elevations of Körberbreen and Petersbreen was an article by Jania (1987) that included hypsometric profiles of both of these glaciers valid for 1960. Another important cartographic study was a 1 : 10 000 map of the forefield and lower part of the Bungebreen glacier snout by Warsaw geologists based on aerial photographs from 1961 (Ostaficzuk et al., 1982; Dzierżek et al., 1991).

3.1.2   NPI map

The topographic map of Sørkapp Land at the scale of 1 : 100 000 based on infrared aerial images from 1990 was developed by NPI and released in analogue form in 2007. The map presented the general image of the area: relief, permanent watercourses, lakes, glaciers, and elevation points. Since the coverage of the peninsula by image data in the
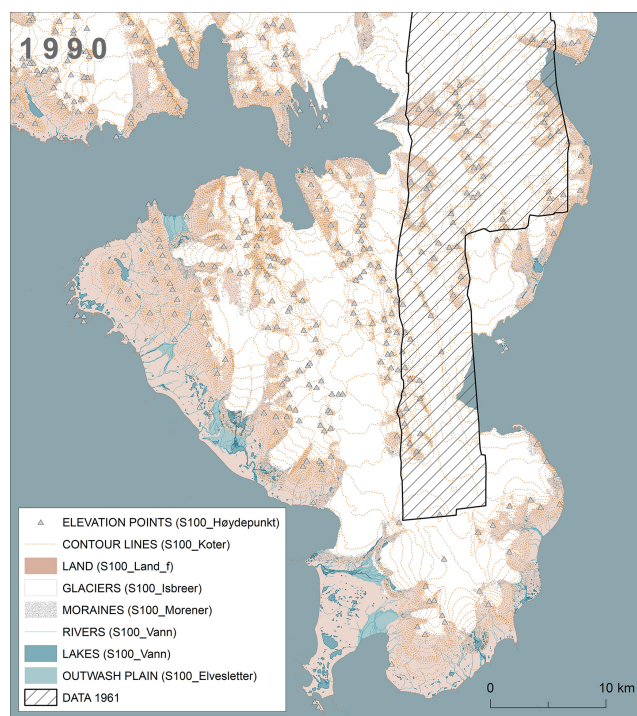
Figure 4. Topographic map of the southern Spitsbergen published in 2007 and released online by NPI (2014).

year 1990 was incomplete in this first dataset (Fig. 2), the gap in the north-eastern part of the peninsula was filled by the data from 1961 (Fig. 4). In 2014, NPI launched a geoportal (https://data.npolar.no, last access: 20 February 2021), enabling spatial data viewing, downloading, and processing. The first online map of the Sørkapp Land peninsula (C13) was available in shapefile format. In the study, the vector layers that present glaciers and elevation points were used.

3.2 Imagery

The image data, consisting mainly of aerial photos captured during the photogrammetric overflights commissioned by the NPI, were used to delineate the extents of the glaciers, as well as visual inspection of the reference DEMs (Fig. 5). The data for 1961 included scans of 14 vertical aerial photos from the historical photogrammetric campaign over the Sørkapp Land area on 24 and 25 August 1961 (Fig. 5a). Black-and-white images at a scale of 1 : 50 000, subjected to photointerpretation, were captured from a ceiling of about 8000 m using a Wild RC camera with a focal length of 153.45 mm (Jania, 1987).

A basis for the delineation of glacier boundaries in 1990 by the NPI consisted of infrared aerial photos at a scale of 1 : 50 000 registered by the RC-10 camera with a focal length of 152 mm. Two stripes for the north-eastern part of the peninsula were missing in the set (Fig. 1); thus, in this study the outlines of four glaciers (Svalisbreen, Sigynbreen,

Grobreen, and Mikaelbreen) were delineated based on the image acquired on 20 August 1990, by the Landsat 5 Thematic Mapper (TM) sensor (Fig. 5b).

The last photogrammetric campaign carried out by the NPI in 2010 covered the entire peninsula (Fig. 1). Photos with a resolution of 0.4 m were captured on 17 August from a ceiling of about 7350 m a.s.l. by the multispectral digital camera UltraCam Xp with a focal length of 100.5 mm. For glacier delineation in 2010 in this study, we used an orthoimage released in 2020 by the NPI (Fig. 5c).

3.3 DEMs

A baseline elevation dataset used for the analysis of map accuracy and changes in glacier thickness consisted of digital elevation models (DEMs) elaborated by the NPI (2014). This study employed a 5 m resolution DEM generated from digital images captured in 2010 and two DEMs with 20 m resolution based on archival aerial photographs acquired by the NPI in 1990 and 1961 (Fig. 6). DEMs were generated using photogrammetric methods based on stereopairs correlation. The vertical accuracy of the DEMs given by the NPI was 2–5 m in non-glacial areas and slightly lower for glacier surfaces (NPI, 2014). The model representing the year 2010, defined by the author as the most accurate, was chosen as a reference dataset throughout the study, and the older models were resampled at a 5 m resolution, which allowed for further compilation with other spatial data.

4 Methods

4.1 Source data processing and evaluation of output data accuracy

4.1.1 Data for 1990

Evaluation of data accuracy produced by NPI for the year 1990 was done by checking the extent to which it fitted existing reliable altitude data for areas not subject to large natural changes over time (in practice, this was the majority of non-glaciated areas). The most reliable source of data for comparisons was the 2010 DEM generated by NPI using photogrammetric methods based on aerial photos and field-measured control points (NPI, 2014). The model from 1990 was validated for horizontal shift against the reference dataset using a procedure developed by Nuth and Kääb (2011) that proposed an analytical solution of a three-dimensional shift vector between two DEMs, by relating the elevation differences to the elevation derivatives of slope and aspect. The correction process was done iteratively until the magnitude of the shift vector approached zero. This method was applied for a terrain that was considered stable and that did not experience changes in geometry over time; when the values of the shift vector were solved, a correction was applied to the whole DEM. Before the correction of the DEM from 2010 versus the DEM from 1990, the magnitude of the shift was
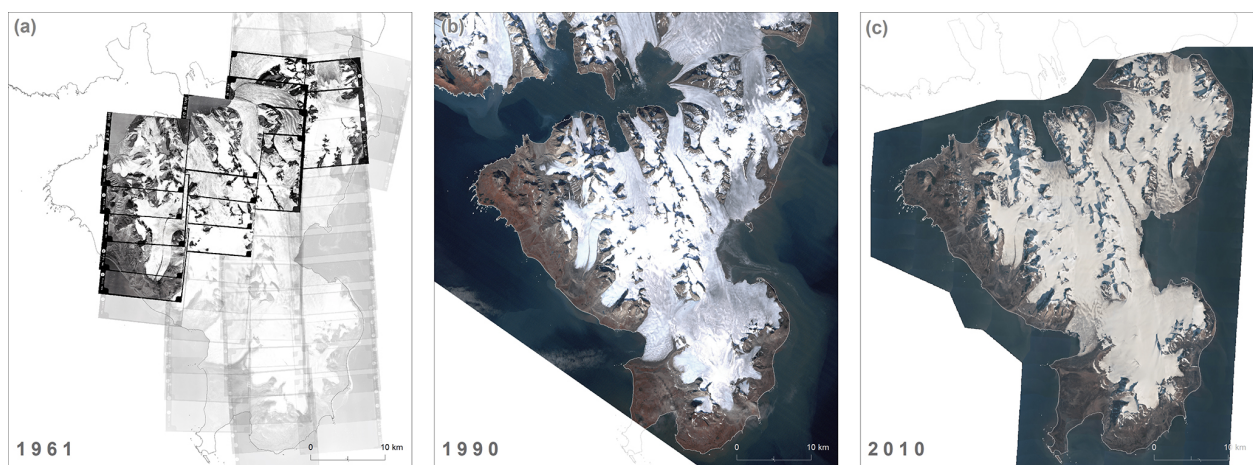
Figure 5. Image data covering Sørkapp Land used in this study: **(a)** aerial photographs from 1961 taken by the NPI on 24 and 25 August 1961; **(b)** Landsat TM5 image captured on 20 August 1990; **(c)** orthophoto created by the NPI (2014) from digital photos captured on 26 August 2010.
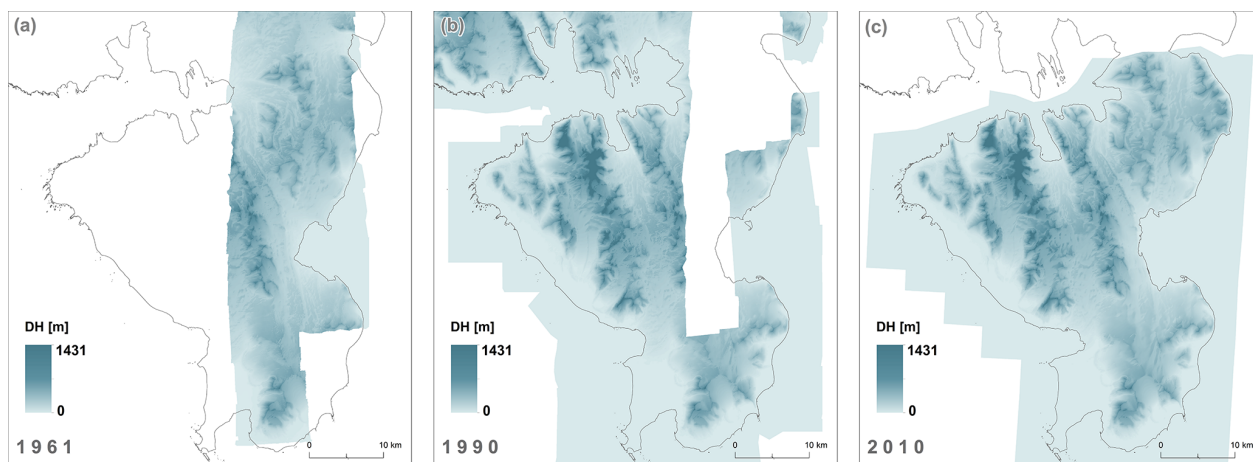

Figure 6. DEMs covering Sørkapp Land generated from aerial photographs by the NPI (2014).

2.14 m in the eastern direction. The mean elevation bias between compared data (z shift component) before the correction was 2.13 m (Fig. 7).

4.1.2 Data for 1961

The maps on which the glacier elevation analysis was based in 1961 in the north-west of Sørkapp Land were processed in several steps using ESRI ArcGIS and MATLAB software (Fig. 8). The analogue maps were first scanned and converted to TIFF format and then defined in the UTM projection, based on a European Datum 1950 (ED50) ellipsoid, in which the background maps had been developed. Subsequently, the coordinate system was converted, and the UTM projection was adopted into the ETRS89 reference system. This allowed for cartographic compilation and integration with other data used for spatial analyses.

Georeferenced maps were used to generate contour lines and vector layers showing the hydrographic network (rivers and lakes), as well as peaks and other elevation points. For this purpose, the raster cleanup and automatic vectorisation functions available in the Arc Scan extension were used. This tool proved very useful for converting raster maps to vector format, as it allowed for significantly faster digitisation of contour lines (for western Sørkapp Land, with its very diversified relief, they were very densely packed – every 5 or 10 m – in the altitude range from 0 up to 1430 m a.s.l.). In the next step, control over the quality of the final result was carried out, and the generated features were manually edited and merged (Fig. 9). Georeferenced geographic information system (GIS) layers – contours, peaks, and topographic points – were supplemented with information about the elevation in the attribute table. Subsequently, contours were converted to
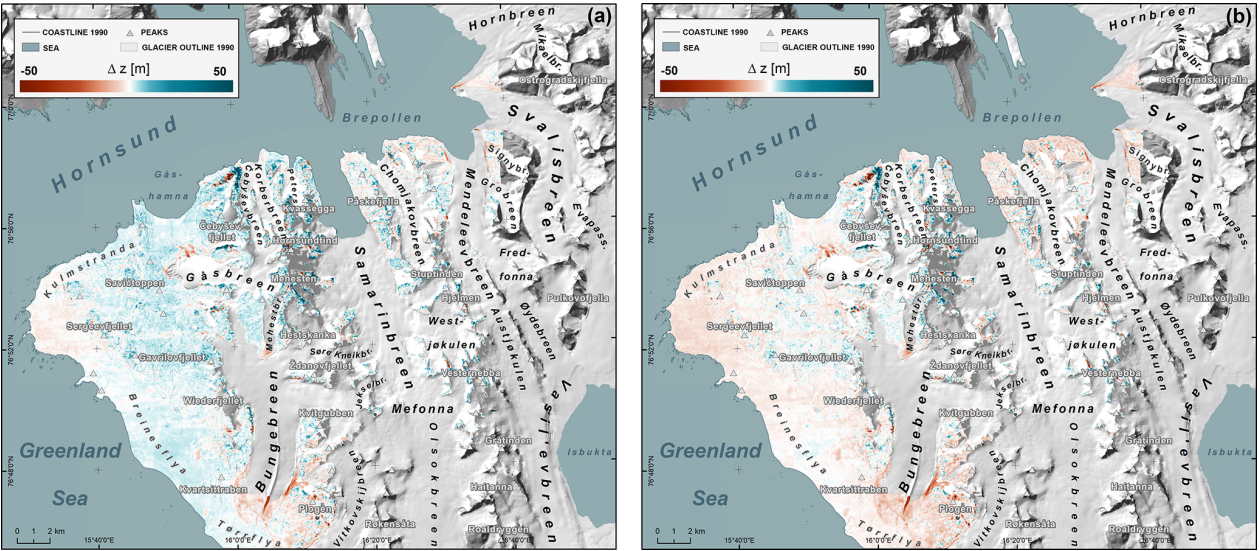
Figure 7. Elevation differences between the 1990 DEM and the 2010 DEM generated by NPI (2014); **(a)** before applying correction; **(b)** after correcting for shift vector as proposed by Nuth and Kääb (2011).

elevation points with a 5 m spatial distance along the lines and merged with layers of peaks and topographic points.

The final step was to verify the relative accuracy of the elevation data obtained. The model representing the year 2010 was chosen as a reference dataset for comparisons and data validation. The easiest way to verify the differences between the two datasets was to subtract one from the other and then interpolate the difference map as proposed by McNabb et al. (2019). A layer of the elevation difference between the datasets was saved as a shapefile that was subsequently used to generate a triangulated irregular network (TIN). In the next step, this model was transformed into a regular grid at a spatial resolution of 5 m. The DEM of difference (DoD) obtained is shown in Fig. 10a.

The first result of the comparison was not satisfactory. In the western part of the DoD, there were large negative values on slopes with eastern exposure, along with large positive values on western slopes, indicating that the two datasets were horizontally offset in relation to each other (Nuth and Kääb, 2011).

In order to define the horizontal shift between two datasets, a procedure developed by Nuth and Kääb (2011) was applied to each sheet separately. The results, as presented in Table 2 and Fig. 10b, indicated that the shift vector was not uniform for all maps in the series. Moreover, although the algorithm permitted improvement of the position of data for 1961 and diminishing of the horizontal errors, on the peripheries of each map sheet the shift between both datasets was still indicated by elevation differences on the slopes (Fig. 10b).

In view of this result, it was attempted to estimate the position errors of the IGF PAN vector layers and then correct them. In the first stage, the locations of the elevation points were assessed. The analysis was performed for each of the

Table 2. Shift vector between data from 1961 and 2010 calculated using a procedure developed by Nuth and Kääb (2011).

Map	Land	Mask	Mask	Shift (m)		
Sheet	(km^2)	(km^2)	(%)	x	y	z
3	18.5	3.0	16.2	−7.59	10.60	−2.42
5	29.6	9.8	33.1	−32.40	−5.68	0.57
6	119.9	24.2	20.2	−28.13	27.66	−2.75
7	15.8	11.2	71.0	3.02	8.19	−0.96
8	155.4	65.3	42.1	−46.98	19.77	−1.44
9	143.4	14.2	9.9	−24.76	23.24	3.38
10	113.7	63.6	55.9	−31.61	32.72	−2.85

sheets separately. The maps shared 189 points representing the same places, of which 27 were triangulation points. The remaining elevation points were mainly peaks, but some indicated geographical features in the field. For the purposes of this study, both types of points were assigned to a common category of objects called "topographic points" (Fig. 9). Furthermore, several topographic points (including points showing the position of building Camp Erna and Konstantinovka) were added in order to match both datasets. Differences in their position in relation to each other are presented in the Supplement table.

From the IGF PAN map series, two sheets (no. 8, Gåsbreen, and no. 9, Samarinbreen) covered the interior of the study area, the adjacent further two sheets (no. 6, Brepollen, and no. 10, Bungebreen) showed less land, and the remaining two sheets (no. 3, Hornbreen, and no. 5, Hornsund) were on the peripheries of the study area. Below is the description of each map sheet used in ascending order.
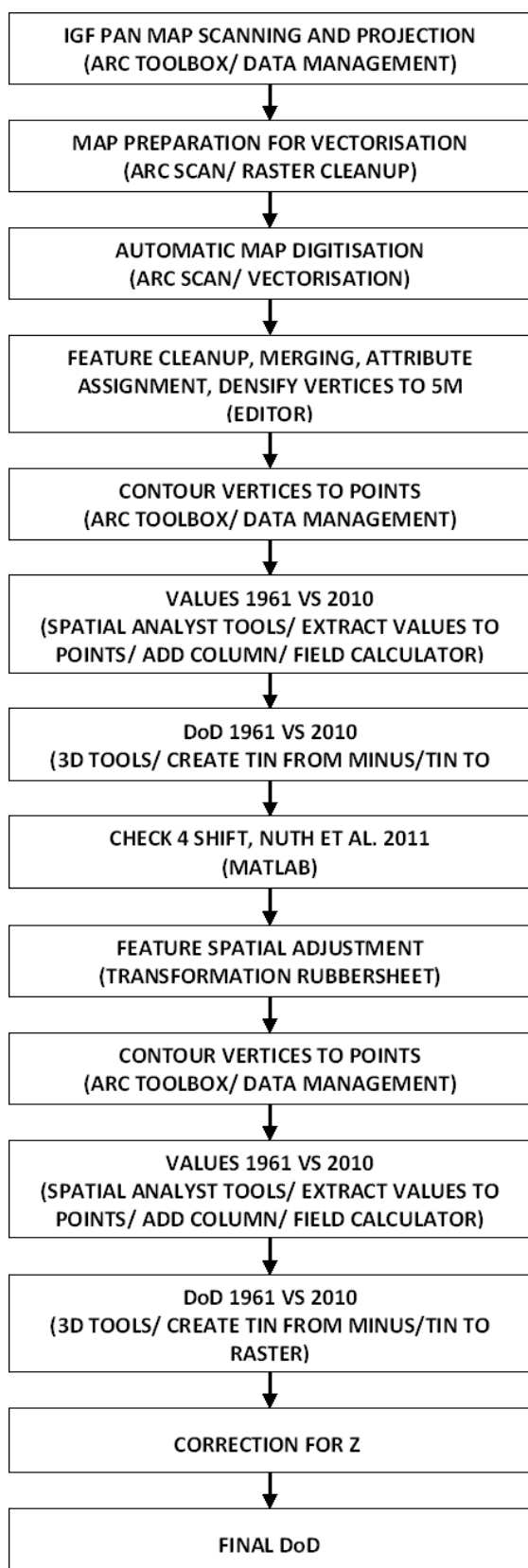
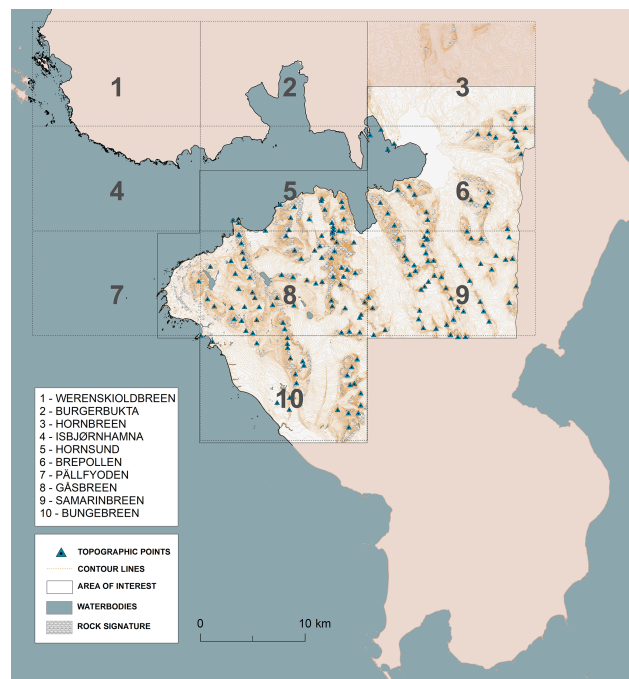**Figure 8.** Workflow for processing IGF PAN map sheets.

Figure 9. Contours and topographic points of map sheets used in the study.

Map sheet no. 3 (Hornbreen), covering the northernmost part of the study area adjacent to the glaciated isthmus, overlapped with the data for 2010 only to a small extent; Fig. 9 shows the southern part of the map that was useful in this study and the three points on which the sheet registration was based.

Similarly for the next IGF PAN map sheet (No. 5 – Hornsund), showing the north-western peripheries of the study area, only the southern part was used. The map sheet contained 18 elevation points which constituted the basis for registration. Figure 9 shows their position and distribution.

Map sheet no. 6 (Brepollen) showed areas further east with Brepollen bay and the fronts of three large tidewater glaciers. On this sheet, 34 points were used to match the NPI dataset. Due to the difficult accessibility of this area, only one of them constituted a triangulation point (Fig. 9).

Map sheet no. 8 (Gåsbreen), which covers the largest area of the peninsula, contained 85 elevation points, which were used for map registration (Fig. 9). Comparing the location of individual points, it can be concluded that the 1961 Gåsbreen map sheet was shifted south-eastward relative to the 2010 NPI data. The peaks of the mountain massifs around Hornsundtind were reproduced the most accurately. Moving westward from Hornsundtind, the distance between the topographic points on both maps increased, which led to the assumption that this was not a simple shift between maps but rather that the problem is a distortion resulting from, among other things, coordinates on the mapping grid being marked incorrectly. The possibility of this problem was already indi-
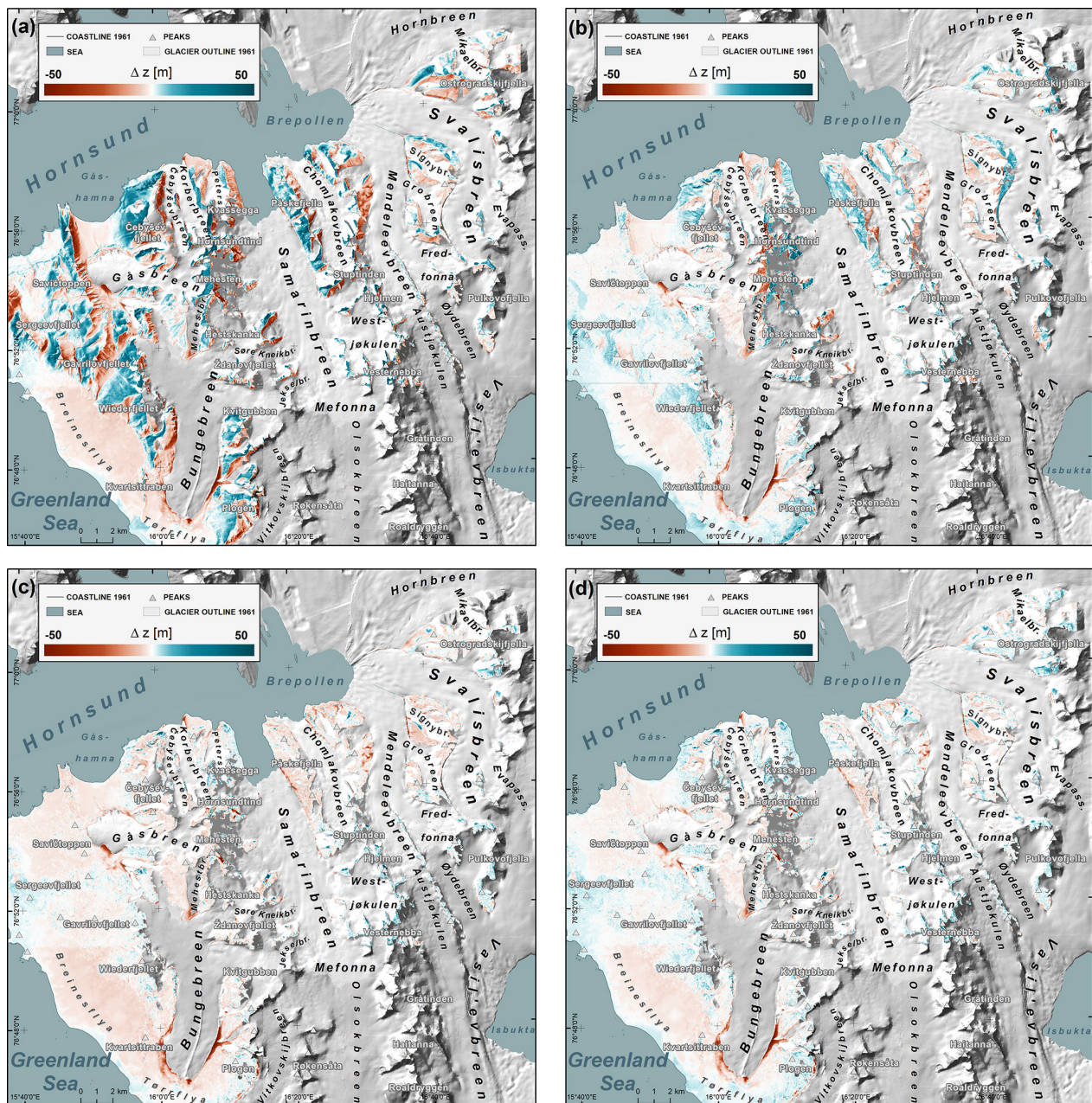
Figure 10. Elevation differences between the 1961 vector layers generated from IGF PAN maps issued in 1987 and the 2010 DEM generated by NPI (2014); **(a)** map rectification based on the nodes of the cartographic grid; **(b)** DEM corrected using method by Nuth and Kääb (2011); **(c)** data rectification based on elevation points **(d)** final DoD.

cated in the description of the IGF PAN map sheets, which explained that the UTM geographic coordinates obtained from NPI that it used differ from the geographic coordinates obtained from astronomical measurements (Barna and Warchoł, 1987).

The next map sheet (no. 9, Samarinbreen) showed the adjacent areas to the east – a large tidewater glacier Samarinbreen and the accumulation zones of Mendeleevbreen and Svalisbreen. The glaciers were separated by very steep

mountain ranges with numerous peaks. The map sheet included 47 elevation points distributed relatively evenly, which could be used for registration. All the points on the map sheet were in the category of topographic points (Fig. 9).

The last corrected sheet of the 1961 map – no. 10, Bungebreen – showed much less land and hence fewer elevation points (Fig. 9). A preliminary assessment of map quality determined a shift in the topographic point layer relative to the contour lines, which most likely occurred while the map was

being prepared for printing. To solve this problem, before
registering the sheet under development, the two digitised
layers were matched against each other so that the eleva-
tion points fell within the contours delineating the summits
(Fig. 9).

In addition to the small number of elevation points and
their shifting relative to contour lines, the planned map reg-
istration was further hampered by the uneven distribution of
elevation points within the sheet. Most of the points were
located on the peaks of mountain massifs in the northern
and eastern parts of the map, while the points in the coastal
zone in the west were missing. The corresponding portion
of the map issued by the NPI for 1990 contained one topo-
graphic point at the base of cape Rafenodden at an altitude
of 17 m a.s.l. To match the 1961 and 1990 data, one point
was added to the Bungebreen sheet, within a small elevation
delimited by a contour at 17.5 m a.s.l. In the next step, the
vector layer of topographic points for 1961 was made denser
by adding a few points at the peaks of four massifs. These
were points within contours delineating the summits of Ark-
fjellet, Plogen, Wiederfjellet, and Stupryggen. The Supple-
ment table shows the coordinates of all points on which the
registration of sheet no. 10 (Bungebreen) was based.

4.2   Fitting data from 1961 and 2010

To align the 1961 vector layers with the 2010 data, they were
registered ("Spatial adjustment" function and "Rubbersheet"
conversion), this time based on triangulation and topographic
points (Supplement table). The vector data thus processed
were then used to generate a DoD with a resolution of 5 m,
similarly as in the first step of data processing (Fig. 8).

A preliminary visual analysis of the DoD obtained
(Fig. 10c) led us to conclude that a significant improvement
had been achieved in terms of the spatial fit of the models.
This was also indicated by a visual assessment of the com-
parative courses and positions of the 1961 and 1990 contours
(Figs. 11–13). Considering the limited possibility of accu-
rately determining the elevation points on which the data reg-
istration for 1961 was based, the results of comparing both
vector layers and both elevation models were considered sat-
isfactory.

4.3   Final elevation model for 1961

After correcting all vector data that were based on the IGF
PAN map sheets and the DoD processed from them, the ac-
curacy of the end product and its adjustment to the remain-
ing reference elevation data were evaluated. To this end, the
final 1961 IGF PAN elevation model was subtracted from the
2010 NPI model, and elevation differences between the mod-
els in non-glaciated areas were analysed in individual slope
classes.

To assess the usefulness of the DEM in studying changes
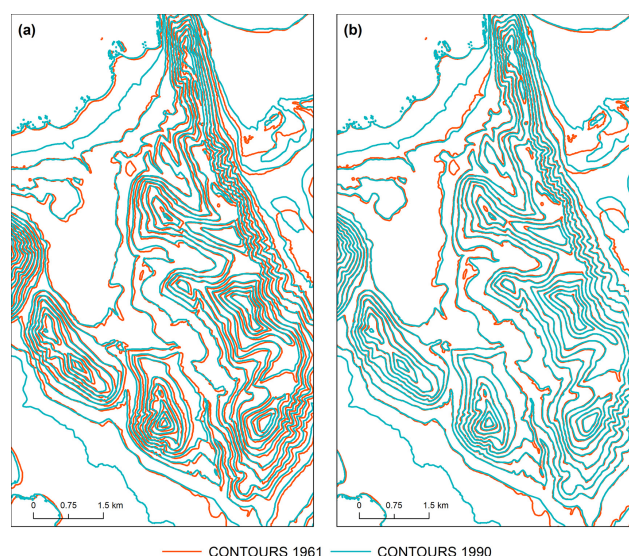in glacier thickness, it can be assumed that its vertical accu-

Figure 11. Course of contour lines in the western part of sheet 8 –
Gåsbreen: georeference based on: **(a)** grid nodes; and **(b)** elevation
points.

racy for non-glacial areas with a slope of less than 30° will
also apply to the surface of most glaciers, because their slope
usually falls into this class. The analysis in the following will
therefore focus on such areas. Apart from the surface of steep
slopes, the evaluation also excludes non-glaciated areas that
cannot be considered stable, because the differences in el-
evation between the two models may result from processes
going on in the natural environment, e.g. melting of dead ice
in marginal zones of glaciers, or the accumulation or ero-
sion activity of proglacial streams in their forefields. Areas
of steep or very steep slopes presented on the IGF PAN maps
as a rock signature also could not be verified.

After considering the aforementioned criteria, evaluation
for vertical shift was performed for each map sheet. The
part of the IGF PAN model selected for the vertical error
analysis covered 88.1 km^2, which constituted 37.3 % of non-
glaciated areas (236.3 km^2) and 14 % of the entire land area
(632.3 km^2) analysed within this model. For comparison, the
area covered by glaciers was 396.0 km^2 (62.6 % of the stud-
ied land area), and the area of steep and very steep slopes was
139.8 km^2 (22.1 %).

Verification of the vertical error of the 1961 model be-
gan with classification of slopes by gradient. To this end, a
slope map was first created and then reclassified to distin-
guish two slope classes for the area: 0–30 and > 30°. Next,
the reclassified raster was transformed to a vector layer, from
which polygons of the second slope class (steep and very
steep slopes) were removed, as were glacier surfaces (extent
from 1961), marginal zones, extra-marginal sandurs, glacial
riverbeds, lakes, and seas. The resulting mask was used to se-
lect areas of elevation differences between the years 1961 and
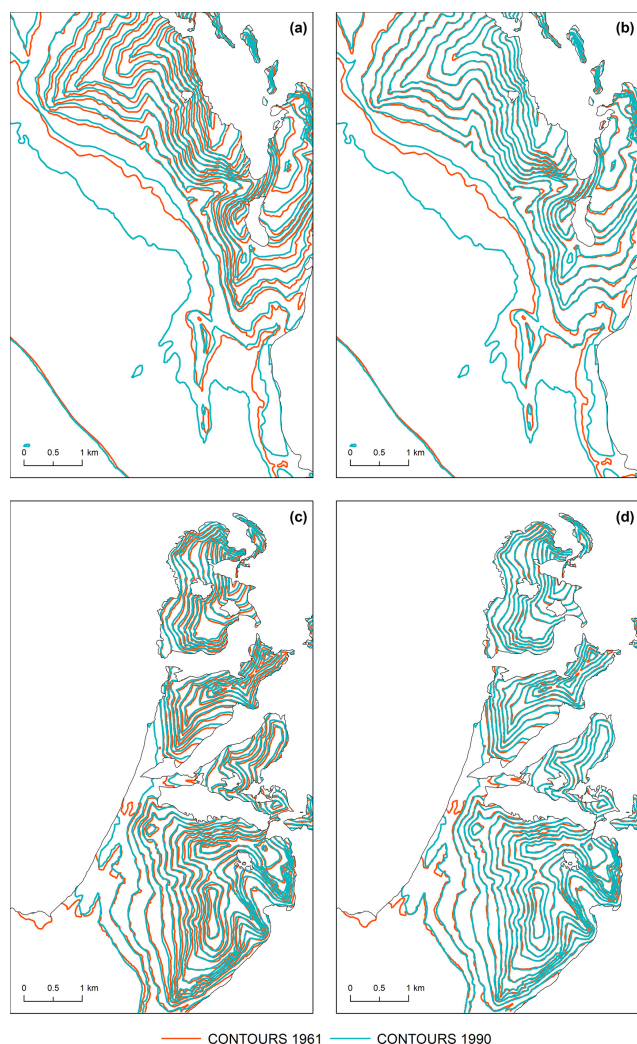2010 from the raster, and these areas were those that would

Figure 13. Course of contour lines in non-glaciated areas in the southern part of sheet no. 5 (Hornsund): georeference based on **(a)** nodes of the cartographic grid and **(b)** elevation points.

analysed sheets of the 1961 map. After initial classification into two glacier types (land-terminating and tidewater), changes in their geometry were calculated.

5 Results

In the study period, most glaciers on the mainland of northwestern Sørkapp Land were in recession, as reflected in a decrease in the total area of nearly 7.2 % – from 74.8 km^2 in 1961 to about 69.4 km^2 in 2010. The average rate of change in the surface area of the region's land-terminating glaciers was 0.19 km^2, i.e. about 0.2 % of glaciated area per year (Table 3).

The pace of surface recession on western Sørkapp Land during the study period 1961–1990 varied between individual land-terminating glaciers. In terms of surface area and ice mass loss, the recession was greatest for the largest glaciers in the region: Gåsbreen and Bungebreen. For these glaciers, the changes are most pronounced in the lower parts of their snouts (Table 3, Fig. 14).

Of the largest glaciers in the region, though in retreat, the snout of the westernmost glacier (Gåsbreen) was in 1961 still piled up on the eastern slopes of the Wurmbrandegga–Savičtoppen ridge to an elevation of 150 m a.s.l. In the period 1961–1990, Gåsbreen's recession manifested itself primarily as a narrowing and thinning of the lowest parts of the glacier with areal decrease by 1.65 km^2, while the frontal retreat was relatively small, amounting to about 320 m (11 m yr^{-1}). Meanwhile, its frontal part was significantly lowered by up to 83 m at the line of its 1990 extent. Outside the frontal and lateral parts, the lowering of the glacier surface gradually became less intense upward, while thickening was observed in the accumulation zone. In the years 1990–2010, the decrease in glacier area continued to progress, reaching

Figure 12. Course of contour lines in non-glaciated areas in the western part of sheet no. 10 (Bungebreen): georeference based on **(a, c)** nodes of the cartographic grid and **(b, d)** elevation points.

be evaluated in terms of vertical accuracy. In the last step, this model was corrected by subtracting the mean difference obtained for each map sheet. After correction, all maps sheets were merged. The final mean elevation difference (bias) between the compared models on stable terrain was 0.0 m, the mean absolute error (MAE) was 2.66 m, and the standard deviation of differences was 2.93 m. The results of comparisons of the final 1961 model against the 2010 reference model are presented in Fig. 10d.

4.4 1961–1990–2010 changes in glacier geometries

The measure to examine the extent and pattern of glacier retreat in the years 1961–1990–2010 was changes in their surface area, the rate of frontal recession, and (where data allowed, i.e. for land-terminating glaciers) changes in thickness. This analysis covered 28 glaciers that lay within the
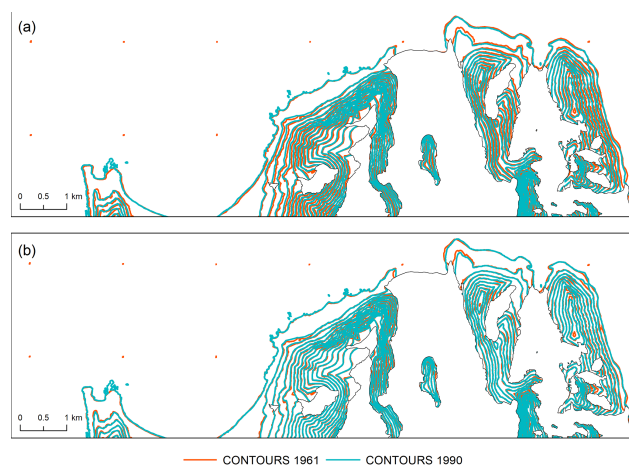
Table 3. Differences in the area of land-terminating glaciers in north-western Sørkapp Land, 1961–1990–2010.

Glacier	Area (km²)			Area change (km²) (%)			Area change rate (km² yr⁻¹) (%)		
	1961	1990	2010	1961–1990	1990–2010	1961–2010	1961–1990	1990–2010	1961–2010
Arkfjellbreen	0.78	0.73	0.67	−0.05 (−6.4)	−0.06 (−8.2)	−0.11 (−14.1)	−0.002 (−0.2)	−0.003 (−0.4)	−0.002 (−0.3)
Bautabreen	0.84	0.78	0.61	−0.06 (−7.1)	−0.17 (−21.8)	−0.23 (−27.4)	−0.002 (−0.3)	−0.009 (−1.1)	−0.005 (−0.6)
Bungebreen	49.61	46.63	43.56	−2.98 (−6.0)	−3.07 (−6.6)	−6.05 (−12.2)	−0.103 (−0.2)	−0.15 (−0.3)	−0.123 (−0.3)
Gåsbreen	13.99	12.34	11.38	−1.65 (−11.8)	−0.96 (−7.8)	−2.61 (−18.7)	−0.06 (−0.4)	−0.05 (−0.4)	−0.05 (−0.4)
Goësbreen	1.19	0.94	0.28	−0.25 (−21.0)	−0.7 (−70.2)	−0.9 (−76.5)	−0.009 (−0.7)	−0.3 (−3.5)	−0.02 (−1.6)
Gråkallbreen	0.16	0.14	0.03	−0.02 (−12.5)	−0.11 (−78.6)	−0.13 (−81.3)	−0.001 (−0.4)	−0.005 (−3.9)	−0.003 (−1.7)
Mehestbreen	3.08	3.04	3.01	−0.04 (−1.3)	−0.03 (−1.0)	−0.07 (−2.3)	−0.001 (0.0)	−0.002 (−0.1)	−0.001 (0.0)
Mikaelbreen	3.73	3.72	3.35	−0.01 (−0.3)	−0.37 (−9.9)	−0.38 (−10.2)	0.000 (0.0)	−0.019 (−0.5)	−0.008 (−0.2)
Nigerbreen	0.29	0.26	0.25	−0.03 (−10.3)	−0.01 (−3.8)	−0.04 (−13.8)	−0.001 (−0.4)	−0.001 (−0.2)	−0.001 (−0.3)
Nordfallbreen	0.83	0.80	0.76	−0.03 (−3.6)	−0.04 (−5.0)	−0.07 (−8.4)	−0.001 (−0.1)	−0.002 (−0.3)	−0.001 (−0.2)
Påskefjella gl.	1.15	1.08	1.05	−0.07 (−6.1)	−0.03 (−2.8)	−0.1 (−8.7)	−0.002 (−0.2)	−0.002 (−0.1)	−0.002 (−0.2)
Plogbreen	0.76	0.64	0.60	−0.12 (−15.8)	−0.04 (−6.3)	−0.16 (−21.1)	−0.004 (−0.5)	−0.002 (−0.3)	−0.003 (−0.4)
Portbreen	0.56	0.51	0.34	−0.05 (−8.93)	−0.17 (−33.33)	−0.22 (−39.3)	−0.002 (−0.3)	−0.009 (−1.7)	−0.004 (−0.8)
Reischachbr.	0.35	0.31	0.25	−0.04 (−11.43)	−0.06 (−19.35)	−0.1 (−28.6)	−0.001 (−0.4)	−0.003 (−1.0)	−0.002 (−0.6)
Signybreen	3.33	2.45	1.94	−0.88 (−26.43)	−0.51 (−20.82)	−1.39 (−41.7)	−0.030 (−0.9)	−0.026 (−1.0)	−0.028 (−0.9)
Silesiabreen	0.24	0.22	0.20	−0.02 (−8.33)	−0.02 (−9.09)	−0.04 (−16.7)	−0.001 (−0.3)	−0.001 (−0.5)	−0.001 (−0.3)
Smaleggbreen	1.94	1.42	1.08	−0.52 (−26.80)	−0.34 (−23.94)	−0.86 (−44.3)	−0.018 (−0.9)	−0.017 (−1.2)	−0.018 (−0.9)
Sokolovbreen	0.96	0.92	0.85	−0.04 (−4.17)	−0.07 (−7.61)	−0.11 (−11.5)	−0.001 (−0.1)	−0.004 (−0.4)	−0.002 (−0.2)
Svalisbreen tr.	1.68	1.37	0.96	−0.31 (−18.45)	−0.41 (−29.93)	−0.72 (−42.9)	−0.011 (−0.6)	−0.021 (−1.5)	−0.015 (−0.9)
Wiederbreen	2.03	1.87	1.73	−0.16 (−7.88)	−0.14 (−7.49)	−0.3 (−14.8)	−0.006 (−0.3)	−0.007 (−0.4)	−0.006 (−0.3)
Total	87.5	80.2	72.9	−7.3 (8.4)	−7.3 (9.1)	14.6 (16.7)			

0.96 km². The manner of the recession changed in this period, which was reflected in a significant shortening of the glacial tongue by 717 m (35.9 m yr⁻¹) and its slightly less-intense lowering than in the previous period, with a maximum of 57 m.

Similar patterns of change in geometry (expressed as thickness increasing in the accumulation zone and decreasing in the ablation zone, combined with a clear retreat of the terminus) were observed for Bungebreen. In the period 1961–1990, the glacier area decreased by 2.9 km², and the frontal retreat was over 1300 m (46 m yr⁻¹). The changes in glacier extent were accompanied by a severe lowering of the surface of the lower parts of the snout of up to 85 m at the line of its extent in 1990. However, against this background, the area of medial moraine stood out, as it played a protective role and attenuated the surface lowering. Here and there, the upper parts of the glacier built up during this period. Because Bungebreen is a compound valley glacier, supplied by several firn fields; this building-up was not uniform throughout the accumulation zone. An increase in glacier thickness of up to 20 m was recorded primarily in parts with a favourable topographic setting, i.e. where ablation is limited by a northern exposure or by being shaded by the steep slopes of the Gråkallen, Kalksteinstupa, and Stupryggen massifs. There was also an approximately 10 m increase in thickness in the ice flowing northward from the Kvitgubben and Lysentoppen massifs. On the contrary, zero or slightly negative values were recorded in the upper southerly-exposed parts of the ice-filled passes on Hestskankfallet and Vasil'evskaret, although there was also a small area of increased thickness

here (Fig. 14a). The accumulation of a large mass of snow in the upper part of the glacier, with a simultaneous decrease in thickness in its lower parts, leads to the fact that it becomes steeper, resulting in a slow increase in stress and, consequently, acceleration of movement. In 2007, when the thickness of the ice layer in the upper part of Bungebreen reached a critical value, a glacier surge was triggered (Sund et al., 2009). The mass of ice accumulated over the years moved downward as a kinematic wave, causing large changes in the geometry of the glacier. Rapid drainage of ice from the reservoir zone led to its reduction in several places to about 30–31 m, while in the lower parts there was an increase in the thickness of the glacial tongue by about 22 m. The acceleration of the glacier's movement was accompanied by its advance. In 2007, Bungebreen's front moved 112 m. This process continued in the following years, reaching an additional 187 m in 2007–2010.

In the years 1961–2010, a very large percentage of area loss was also observed in the western and low-lying small-valley Gråkallbreen, Goësbreen, and Portbreen glaciers. This process was accompanied by significant thinning, often along the longitudinal profile, and totalled 20–40 m in the upper parts and 40–60 m at their termini. The decrease in thickness was very clearly marked in these glaciers, especially in the central and lower parts, which in the case of the Portbreen glacier, for example, led to the ice cover partially disappearing and fragmenting into smaller ice lobes separated by a rock step (Fig. 14c).

Against the backdrop of glaciers that have undergone significant changes over the analysed decades (seen mainly in a
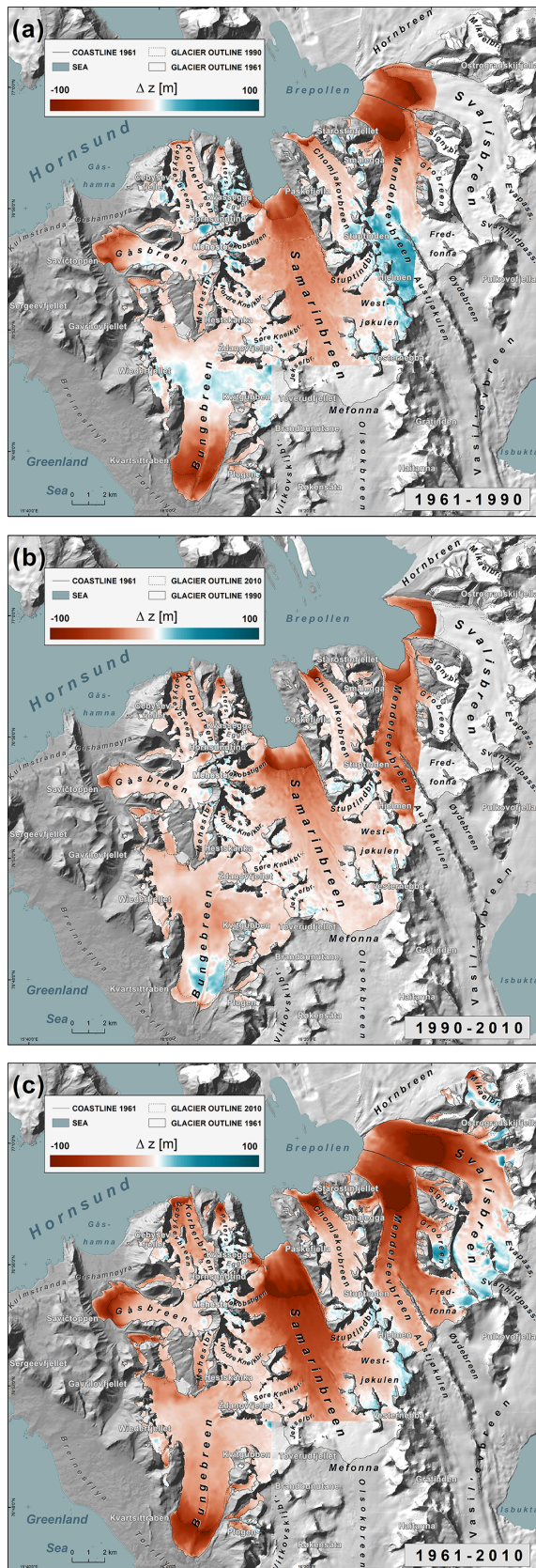
Figure 14. Glacier elevation change in the north-western Sørkapp Land, 1961–1990–2010: **(a)** 1961–1990; **(b)** 1990–2010; **(c)** 1961–2010.

significant loss of ice mass), two glaciers stand out as having undergone relatively little change in geometry. These are the Nordfallbreen and Mehestbreen glaciers. Between 1961 and 2010, the Nordfallbreen area decreased by only 0.07 km^2, i.e. 8.4 %, which is among the lowest values in the entire region (Table 3). The extent of the glacier went virtually unchanged in 1961–1990. Only after 1990 did Nordfallbreen slightly retreat, losing 38 m of its length. However, the slight changes in surface area and extent were accompanied by a thinning. This was less than in other glaciers in the region and ranged from 20–30 m in the ablation zone to 8–13 m in the accumulation zone (Fig. 14). Even smaller changes in geometry were recorded for the Mehestbreen. During the entire study period, its area decreased only by 0.07 km^2 (i.e. 2.3 %), and the glacier terminus receded by 120 m in 1961–1990, while in the next research period, 1990–2010, it was only about 10 m (Table 3). Analysis of elevation differences in the glacier longitudinal profile reveals that thinning in the years 1961–1990 was greatest in the lower parts of the ablation zone, at 30–40 m, while the accumulation zone actually increased in thickness by about 10–15 m (Fig. 14c).

In the north of the area, which is dominated by glaciers flowing into the Hornsund fjord, the disappearance of the ice cover was mainly the result of iceberg calving. The surface area of the eight analysed calving glaciers fell from 210 km^2 in 1961 to 177 km^2 in 2010, constituting a 15.9 % decrease (Table 4). The average recession rate of the calving glaciers in 1961–2010 was 0.01 % yr^{-1}. For the region's largest glaciers on the west, which flow directly into the Hornsund fjord (i.e. Körberbreen and Petersbreen), the areal decrease was 7 %–9 %, while for the largest glaciers further east it was much larger at 22 %–26 %. Smaller glaciers calving into Samarinvågen bay, lost from 13 % in Kvasseggbreen to 16.6 % in Eggbreen (Table 3).

Changes in surface area were accompanied by changes in ice thickness. In their ablation zones, which are subject to greater insolation, the thickness decreased, and a general frontal retreat was observed. This differed in size and pace for individual glaciers (Fig. 14, Tables 4 and 5). In the case of the Körberbreen glacier, the maximum lowering of the frontal parts (between the 1984 and 2010 extents) did not exceed 100 m. However, further eastward in the former tributaries of the Samarinbreen and in Petersbreen this lowering was greater, reaching 105 m for the Kvasseggbreen snout, 120 m in parts of the Eggbreen, and up to as much as 125 m in Peterbreen. In the higher parts of the glaciers studied, there was a clear build-up of firn fields in this period. In the east, in the largest calving glaciers of the study area, Mendeleevbreen and Svalisbreen, this lowering reached as much as 120 m (Fig. 14).

Table 4. Differences in the area of tidewater glaciers in north-western Sørkapp Land, 1961–1990–2010.

Glacier	Area (km²)			Area change (km²) (%)			Area change rate (km² yr⁻¹) (%)		
	1961	1990	2010	1961–1990	1990–2010	1961–2010	1961–1990	1990–2010	1961–2010
Körber	10.8	10.5	10.0	−0.25 (−2.32)	−0.55 (−5.22)	−0.80 (−7.41)	−0.01 (−0.08)	−0.03 (−0.26)	−0.02 (−0.002)
Peters	2.3	2.2	2.1	−0.07 (−3.03)	−0.12 (−5.36)	−0.19 (−8.23)	−0.002 (−0.10)	−0.01 (−0.27)	−0.004 (−0.002)
Kvassegga	0.9	0.8	0.8	−0.09 (−10.11)	−0.03 (−3.75)	−0.12 (−13.48)	−0.003 (−0.35)	−0.002 (−0.19)	−0.002 (−0.01)
Egg	2.3	1.9	1.9	−0.35 (−15.28)	−0.03 (−1.55)	−0.38 (−16.59)	−0.01 (−0.53)	−0.002 (−0.08)	−0.01 (−0.01)
Samarin	86.6	82.9	78.5	−3.32 (−3.85)	−4.47 (−5.39)	−7.79 (−9.03)	−0.11 (−0.13)	−0.22 (−0.27)	−0.16 (−0.003)
Chomjakov	15.3	14.5	14.0	−0.83 (−5.41)	−0.52 (−3.59)	−1.35 (−8.81)	−0.03 (−0.19)	−0.03 (−0.18)	−0.03 (−0.004)
Mendeleev	45.2	38.5	35.0	−6.67 (−14.77)	−3.50 (−9.10)	−10.17 (−22.52)	−0.23 (−0.51)	−0.18 (−0.45)	−0.21 (−0.01)
Svalis	47.0	41.4	34.5	−5.58 (−11.87)	−6.96 (−16.81)	−12.54 (−26.69)	−0.19 (−0.41)	−0.35 (−0.84)	−0.26 (−0.01)
Total	210.0	192.8	176.7	−17.16 (−8.17)	−16.18 (−8.39)	−33.34 (−15.88)	−0.59 (−0.28)	−0.81 (−0.42)	−0.68 (−0.01)

Table 5. Surface elevation change of the glaciers in north-western Sørkapp Land, 1961–2010.

Glacier	Mean elevation change rate (m yr⁻¹)
Arkfjellbreen	−0.40 ± 0.05
Bautabreen	−0.16 ± 0.05
Bungebreen	−0.51 ± 0.05
Chomjakovbreen	−0.39 ± 0.05
Eggbreen	−0.42 ± 0.05
Gåsbreen	−0.17 ± 0.05
Goësbreen	−0.68 ± 0.05
Gråkallbreen	−0.44 ± 0.05
Körberbreen	−0.42 ± 0.05
Kvasseggbreen	−0.11 ± 0.05
Mehestbreen	−0.36 ± 0.05
Mendeleevbreen	−0.71 ± 0.05
Mikaelbreen	−0.17 ± 0.05
Nigerbreen	−0.20 ± 0.05
Nordfallbreen	−0.38 ± 0.05
Påskefjella gl.	−0.06 ± 0.05
Petersbreen	−0.35 ± 0.05
Plogbreen	−0.35 ± 0.05
Portbreen	−0.41 ± 0.05
Reischachbr.	0.35 ± 0.05
Samarinbreen	−0.62 ± 0.05
Signybreen	−0.40 ± 0.05
Silesiabreen	−0.17 ± 0.05
Smaleggbreen	−0.36 ± 0.05
Sokolovbreen	−0.46 ± 0.05
Svalisbreen	−0.67 ± 0.05
Svalisbreen tr.	−0.26 ± 0.05
Wiederbreen	−0.23 ± 0.05
All glaciers	−0.56 ± 0.05

6　Discussion

The accuracy of simulations prognosing changes in glacier volumes based on dynamics models depends largely on the prerequisite that those models have been initialised correctly (Oerlemans, 1997; Collao-Barrios et al., 2018). Glaciers differ in response time to changes in mass balance, and this requires that data on the geometry of glaciers should go back as far as possible – preferably to a state of equilibrium with climatic conditions (Zekollari et al., 2020). If this is not possible, these models can be properly calibrated and verified using later data; nevertheless, the further back the data go, the better and the more accurately future changes can be predicted. Thus, any glacier topography data from the 1960s are extremely valuable (Andreassen et al., 2020). There is little data available for the Svalbard region in this period, highlighting the importance of the results presented here.

The disappearance of ice in the western Sørkapp Land in 1961–2010 was the result of various processes. It was caused by both surface melting of ice and the breaking-off of icebergs during calving. Both processes had a significant impact on the overall mass loss from the glaciers on Sørkapp Land. They are estimated to be responsible for 79 % and 21 %, respectively, of the overall mass loss from glaciers across Svalbard (Błaszczyk et al., 2009).

Important factors influencing the ablation of glaciers flowing into the Hornsund fjord in the western part of the Sørkapp Land peninsula are the northern and eastern exposures of their accumulation zones and the significant shading of their surfaces by high mountain ranges. For this reason, the winter snow cover here lasts longer and is thicker, and the ablation is weaker relative to neighbouring glaciers with western exposures (Jania, 1987). Higher accumulation and some reduction in glacier ablation also result from their accumulation zones reaching more than 700 m a.s.l. and being surrounded by the steep slopes of the massifs that supply them with additional snow (Jania, 1987).

It can be seen that the interaction of all these factors has clearly increased the thickness of firn and ice in the highest and middle parts of the glaciers that flow into the Hornsund fjord during the years 1961–2010 (Fig. 14). At the same time, the changes in position of the thickened parts of the Körberbreen and Petersbreen glaciers are noteworthy, as shown by studies of changes in the range and speed of Körberbreen in shorter time intervals (Pillewizer, 1939; Jania, 1987; Ziaja

and Dudek, 2011; Błaszczyk et al., 2013). This suggests, in line with the supposition of Jania (1987), regular short-term displacement of the kinematic waves of ice that are characteristic of surging (especially in relation to Körberbreen). The research period adopted here (on the order of several decades) is too long to properly detect and illustrate this phenomenon, but other studies for this area provide evidence supporting the thesis.

On land, glacial systems evolved at variable rates, which can be associated with variable topoclimatic and local conditions in the western Sørkapp Land. The recession was fastest in the western and southernmost glaciers of the region, where the air masses of the Greenland Sea and the warm West Spitsbergen Current are in effect (Ziaja et al., 2016). Aside from clear frontal retreat, there was also a significant decrease in thickness in their longitudinal profiles. In the small, westward, low-lying valley glaciers, this was especially pronounced, especially in the middle and lower parts of the snouts, where smaller patches of dead ice emerged.

Although glacial recession was the predominant phenomenon in land-terminating glaciers in western Sørkapp Land, the warming effect was mitigated in some places by the terrain and the significant elevation of the mountain massifs from which some of the glaciers originate. Being favourably located either at a significant elevation or in the shadow of high mountains stabilised the situation somewhat for some glaciers here, because their maintenance or local increase of mass was favoured by both an orographic increase in snowfall and additional supply from avalanches. This applies, for example, to Nordfallbreen, which is shaded from the south, and small glaciers originating on the slopes of the Hornsundtind and Kvassegga groups of mountains.

Nordfallbreen is adjacent to Nordfallet (824 m a.s.l.) to the south, which shades it against the sun while also providing it with additional supply by avalanches. Mehestbreen is similarly fed, being bordered to the east by the Mehesten (1383 m a.s.l.) and Hestskanka (997 m a.s.l.) massifs and by Hoven hill (869 m a.s.l.) to the north. Their influence is seen in the spatial distribution of positive values on the glacier elevation change maps, more of which lie closer to the eastern edge of the glacier. An additional factor limiting ablation on Mehestbreen is its significant elevation, which puts a large part of the glacier's surface above the mass balance equilibrium line (300–400 m a.s.l.).

There are few studies where the results of this study of the peninsula's surface glaciation recession can be compared against. In the older literature, such analyses were carried out for individual glaciers (Jania, 1987; Schöner and Schöner, 1997) or at the regional scale at best (Jania, 1988a). However, the observed trends in the elevations of the Sørkapp Land glaciers in 1961–2010 are comparable to other areas of Spitsbergen, although the number of studies with similar temporal coverage is limited (Nuth et al., 2010; Małecki, 2013; Błaszczyk et al., 2013).

7 Data availability

All data are available at the Zenodo service (https://doi.org/10.5281/zenodo.4573129) (Dudek and Pętlicki, 2021). Data format: ESRI shapefile and GeoTIFF. The datasets contain vector layers (topographic and glacier outlines) and a digital elevation model (DEM) covering the northwestern part of Sørkapp Land peninsula, Svalbard, for the year 1961. The shapefile "glacier_1961_northwestern _Sorkappland.shp" contains the glacier areas manually delineated from vertical aerial photos captured during the historical photogrammetric overflight commissioned by the Norwegian Polar Institute on 24 and 25 August 1961. The shapefile "contour_1961_10m_northwestern_Sorkappland.shp" contains contour lines with intervals of 10 m based on digitised historical maps edited in 1987 by the Institute of Geophysics of the Polish Academy of Sciences and registered using a cartographic grid and elevation points. The shapefile "peak_1961_northwestern_Sorkappland.shp" contains elevation points – topographic and triangulation – used in the vector data registration process. Shapefile "rock_1961_northwestern_Sorkappland.shp" delineates areas very steep presented on the source maps as rock cliff symbols. This file also indicates areas where the highest elevation errors in the generated digital elevation model are plausible. All shapefiles were produced in the UTM projection system (Northern Hemisphere, zone 33) based on the ETRS89 ellipsoid (datum D_ETRS_1989). The raster file "dem_1961_5m_northwestern_Sorkappland.tif" contains a digital elevation model (DEM) with 5 m resolution generated from corrected contour lines.

8 Conclusions

Correctly assessing the utility of the series of maps issued by the Institute of Geophysics of the Polish Academy of Sciences is very important in order to precisely determine changes in glacier geometries in western Sørkapp Land. Although the IGF PAN field campaign was conducted in the early 1980s, the maps published after the expedition were based on elevation data taken from aerial photos from 1961, upon which only glacier extents were updated (with a change in colour of contours). Crucially, contour lines were not updated in this 1984 edition and continued to represent the higher elevations of 1961.

In response to this, the map coordinates on the 1961 map have now been corrected so that they can be used for comparative analyses of changes in glacier surface elevations over the years 1961–1990–2010. This is especially true for glaciers that are land-terminating, for which data relating to their entire surface area are now corrected and complete.

However, the value of data on tidewater glaciers for various types of comparison is limited to their upper parts (above the line of their 1984 extents). This is because updating their extents in 1984 required that contour lines between the ex-

tents designated for 1961 and 1984 be deleted and that the elevation of this surface be zeroed on the map, i.e. brought to sea level. Therefore, when analysing the IGF PAN sheets, it is impossible to determine the exact height of the ice cliffs of the Körberbreen, Petersbreen, Kvasseggbreen, and Eggbreen tidewater glaciers in 1961.

Consequently, this study finds that in the years 1961–2010 the maximum lowering of surface was about 90–100 m in the largest land-terminating glaciers on the peninsula, and over 120 m in tidewater glaciers (above the line marking their 1984 extents), with a mean glacier elevation change rate of $-0.56 \pm 0.05 \, \text{m yr}^{-1}$ over the entire region. Glaciated areas aside, the surface-corrected IGF PAN maps can also be used to analyse landscape dynamics, including changes that occur in marginal zones.

Author contributions. JD conceived the study, processed and analysed the data, and drafted the manuscript. MP contributed to the discussion, review, and editing of the manuscript.

References

Andreassen, L. M., Elvehøy, H., Kjøllmoen, B., and Belart, J. M.: Glacier change in Norway since the 1960s–an overview of mass balance, area, length and surface elevation changes, J. Glaciol., 66, 313–328, https://doi.org/10.1017/jog.2020.10, 2020.

Barna, S. and Warchoł, Z. (Eds.).: Spitsbergen, 1:25 000 – 10 arkuszy, Institute of Geophysics of the Polish Academy of Sciences, Topographic Service of the Polish Army, Institute of Geodesy and Cartography, 1987.

Bhambri, R., Bolch, T., Chaujar, R. K., and Kulshreshtha, S. C.: Glacier changes in the Garhwal Himalaya, India, from 1968 to 2006 based on remote sensing, J. Glaciol., 57, 543–556, https://doi.org/10.3189/002214311796905604, 2011.

Bhattacharya, A., Bolch, T., Mukherjee, K., King, O., Menounos, B., Kapitsa, V., Neckel, N., Yang, W., and Yao, T.: High Mountain Asian glacier response to climate revealed by multi-temporal satellite observations since the 1960s, Nat. Commun., 12, 4133, https://doi.org/10.1038/s41467-021-24180-y, 2021.

Błaszczyk, M., Jania, J. A., and Hagen, J. O.: Tidewater glaciers of Svalbard: Recent changes and estimates of calving fluxes, Pol. Polar Res., 30, 85–142, 2009.

Błaszczyk, M, Jania, J. A., and Kolondra, L.: Fluctuations of tidewater glaciers in Hornsund Fjord (Southern Svalbard) since the beginning of the 20th century, Pol. Polar Res., 34, 327–352, 2013.

Collao-Barrios, G., Gillet-Chaulet, F., Favier, V., Casassa, G., Berthier, E., Dussaillant, I., Mauginot, J., and Rignot, E.: Ice flow modelling to constrain the surface mass balance and ice discharge of San Rafael Glacier, Northern Patagonia Icefield, J. Glaciol., 64, 568–582, https://doi.org/10.1017/jog.2018.46, 2018.

De Geer, G.: Plan öfver det svensk-ryska gradmätningsnätet på Spetsbergen efter nyaste sammanstäld Maj 1900 1:1000000, Mesure D'un Arc de Méridien au Spitzberg, Entr. en 1899–1902, Description Topographique de la Région Exploré, Géologie, Aktiebolaget Centraltryckeriet, Stockholm, Sweden, 1923.

Dowdeswell, J., Hodgkins, R., Nuttall, A. M., Hagen, J. O., and Hamilton, G. S.: Mass balance change as a control on the frequency and occurrence of glacier surges in Svalbard, Norwegian High Arctic, Geophys. Res. Lett., 22, 2909–2912, https://doi.org/10.1029/95GL02821, 1995.

Dudek, J., Współczesne przemiany krajobrazu półwyspu Sørkapp Land (Spitsbergen) pod wpływem recesji lodowców na podstawie danych teledetekcyjnych, Ph.D. thesis, Jagiellonian University, Poland, 294 pp., https://ruj.uj.edu.pl/xmlui/handle/item/77309 (last access: 2 February 2021), 2019 [in Polish].

Dudek, J. and Pętlicki, M.: Topography of the north-western Sørkapp Land (Svalbard) in the year 1961, Zenodo [data set], https://doi.org/10.5281/zenodo.4573129, 2021.

Dzierżek, J., Lindner, L., Marks, L., Nitychoruk, J., and Szczęsny, R.: Application of remote sensing to topographic maps of polar areas, Pol. Polar Res., 12, 149–160, 1991.

Eckerstorfer, M., and Christiansen, H.: The High Arctic maritime snow climate in Central Svalbard, Arct. Antarct. Alp. Res., 43, 11–21, https://doi.org/10.1657/1938-4246-43.1.11, 2011.

Farnsworth, W. R., Ingólfsson, Ó., Retelle, M., and Schomacker, A.: Over 400 previously undocumented Svalbard surge-type glaciers identified, Geomorphology, 264, 52–60, https://doi.org/10.1016/j.geomorph.2016.03.025, 2016.

Finsterwalder, R.: Photogrammetry and glacier research with special reference to glacier retreat in the eastern Alps, J. Glaciol., 2, 306–315, 1954.

Førland E. J., Benestad R., Hanssen-Bauer I., Haugen J. E., and Skaugen T. E.: Temperature and precipitation development at Svalbard 1900–2100, Adv. Meteorol., 2011, 893790, https://doi.org/10.1155/2011/893790, 2011.

Fürst, J. J., Navarro, F., Gillet-Chaulet, F., Huss, M., Moholdt, G., Fettweis, X., Lang, C., Seehaus, T., Ai, S., Benham, T. J., Benn, D. I., Björnsson, H., Dowdeswell, J. A., Grabiec, M., Kohler, J., Lavrentiev, I., Lindbäck, K., Melvold, K., Pettersson, R., Rippin, D., Saintenoy, A., Sánchez-Gámez, P., Schuler, T. V., Sevestre, H., Vasilenko, E., and Braun, M. H.: The ice-free topography of Svalbard, Geophys. Res. Lett., 45, 21, 11760–11769, https://doi.org/10.1029/2018GL079734, 2018.

Geyman, E. C., van Pelt W. J. J., Maloof, A. C., Aas, H. F., and Kohler, J.: Historical glacier change on Svalbard predicts doubling of mass loss by 2100, Nature, 601, 374–379, https://doi.org/10.1038/s41586-021-04314-4, 2022.

Girod, L., Nielsen, N. I., Couderette, F., Nuth, C., and Kääb, A.: Precise DEM extraction from Svalbard using 1936 high oblique imagery, Geosci. Instrum. Method. Data Syst., 7, 277–288, https://doi.org/10.5194/gi-7-277-2018, 2018.

Grabiec M., Ignatiuk I., Jania J. A., Moskalik M., Głowacki P., Błaszczyk M., Budzik T., and Walczowski W.: Coast formation in an Arctic area due to glacier surge and retreat: The Hornbreen-Hambergbreen case from Spistbergen, Earth Surf. Proc. Land., 43, 387–400, https://doi.org/10.1002/esp.4251, 2017.

Hagen, J. O. and Liestøl, O.: Long term glacier mass balance investigations in Svalbard 1950–1988, Ann. Glaciol., 14, 102–106, https://doi.org/10.3189/S0260305500008351, 1990.

Hagen J. O., Liestøl O., Roland E., and Jørgensen T.: Glacier Atlas of Svalbard and Jan Mayen, Norsk Polarinstitutt Meddelelser (Oslo), Norway, 129, 141 pp., ISBN 82-7666-066-5, 1993.

Heintz, A.: Noen iakttagelser over isbreenes tilbakegang i Hornsund, V. Spitsbergen, Norsk Geol. Tidsskr., 31, 7–36, 1953.

Hoel, A.: The Norwegian Svalbard Expeditions 1906–1926, Skrifter om Svalbard og Ishavet, 1, Oslo, https://brage.npolar.no/npolar-xmlui/bitstream/handle/11250/173618/Skrifter001.pdf?sequence=1&isAllowed=y (last access: 29 August 2023), 1929.

Holmlund, E.: Aldegondabreen glacier change since 1910 from structure-from-motion photogrammetry of archived terrestrial and aerial photographs: Utility of a historic archive to obtain century-scale Svalbard glacier mass losses, J. Glaciol., 67, 107–116, https://doi.org/10.1017/jog.2020.89, 2021.

Isachsen, G., Hoel, A., Resvoll Holmsen, H., and Schetelig, J.: Exploration du Nord-Ouest du Spitsberg entreprise sous les auspices de S. A. S. le Prince de Monaco par la Mission Isachsen, I. Récit de voyage, II. Description du champ d'opération, III. Géologie, IV. Les Formations Primitives, 5, Impr. de Monaco, 1912–1914.

Isaksen, K., Nordli, Ø., Førland, E. J., Łupikasza, E., Eastwood, S., and Niedźwiedź, T.: Recent warming on Spitsbergen-Influence of atmospheric circulation and sea ice cover, J. Geophys. Res.-Atmos., 121, 1–19, https://doi.org/10.1002/2016JD025606, 2016.

Jacob, T., Wahr, J., Pfeffer, W. T., and Swenson, S.: Recent contributions of glaciers and ice caps to sea level rise, Nature, 482, 514–518, https://doi.org/10.1038/nature10847, 2012.

James, T. D., Murray, T., Barrand, N. E., Sykes, H. J., Fox, A. J., and King, M. A.: Observations of enhanced thinning in the upper reaches of Svalbard glaciers, The Cryosphere, 6, 1369–1381, https://doi.org/10.5194/tc-6-1369-2012, 2012.

Jania, J. A.: Pomiary ablacji lodowca Nordfall jako element do bilansu masy i energii, Dokumentacja prac w problemie MR. II. 16. B, Institute of Geophysics of the Polish Academy of Sciences, 4, 1979.

Jania, J. A.: Debris forms and processes in Gåsdalen region in photogrammetric investigations and repeated terrestrial photograms, Results of Investigations of the Polish Scientific Spitsbergen Expeditions, Acta Universitatis Wratislaviensis, 4, 96–114, 1982.

Jania, J. A.: Interpretacja glacjologiczna zdjęć lotniczych otoczenia Hornsundu (Spitsbergen) na przykładzie lodowców Körber i Peters, Fotointerpretacja w Geografii, 9, 60–107, 1987.

Jania, J. A.: Dynamiczne procesy glacjalne na południowym Spitsbergenie (w świetle badań fotointerpretacyjnych i fotogrametrycznych), Dynamic Glacial Processes in south Spitsbergen [in the Light of Photointerpretation and Photogrammetric Research], Prace Naukowe Uniwersytetu Śląskiego w Katowicach, 258 pp., ISSN 0208-6336, 1988a.

Jania, J. A.: Klasyfikacja i cechy morfometryczne lodowców otoczenia Hornsundu, Spitsbergen. Wyprawy Polarne Uniwersytetu Śląskiego 1980–1984, Prace Naukowe Uniwersytetu Śląskiego, Katowice, 910, 12–47, 1988b.

Jania, J. A., Kolondra, L., and Aas, H. F.: Orthophotomap 1:25000, Werenskioldbreen and surrounding area, Faculty of Geosciences, University of Silesia and Norsk Polarinstitutt, Sosnowiec and Tromsø, 2002.

Jania, J. A. and Szczypek, T.: Kartowanie geomorfologiczne otoczenia fiordu Hornsund na podstawie interpretacji zdjęć lotniczych, Fotointerpretacja w Geografii, 9, 108–128, 1987.

Jiskoot, H., Murray, T., and Boyle, P.: Controls on the distribution of surge-type glaciers in Svalbard, J. Glaciol., 46, 412–422, https://doi.org/10.3189/172756500781833115, 2000.

Kłysz, P. and Lindner, L.: Evolution of the marginal zone and the forefield of the Bunge Glacier, Spitsbergen, Acta Geol. Pol., 32, 253–266, 1982.

Knight, P. G.: Glacier Science and Environmental Change, Blackwell Science Ltd., Oxford, 527 pp., https://doi.org/10.1002/9780470750636, 2006.

Kolondra, L.: Mapa 1:5000, Wurmbrandegga – fragment wsch. stoku pasma, District Geodetic and Cartographic Enterprise, Katowice, 1979.

Kolondra, L.: Mapa 1:5000, Tsjebysjovfiellet – fragment zach. stoku pasma. District Geodetic and Cartographic Enterprise, Katowice, 1980.

Kolondra, L.: Prace i dorobek polskich fotogrametrów w Arktyce (1934–2000), Archiwum Fotogrametrii, Kartografii i Teledetekcji, 10, 1–14, ISBN 83-906804-4-0, 2000.

Kolondra, L.: Problemy fotogrametrycznego pozyskiwania danych w badaniach glacjologicznych – studium metodyczne na przykładzie Spitsbergenu. Ph.D. thesis, Faculty of Geosciences, University of Silesia, Sosnowiec, 166 pp. + 3 maps, 2002.

Kolondra, L.: Photogrammetry the Authentic Source of Data For Spitsbergen Glaciological Research, Geoinformatica Polonica, Works of the Geoinformatics Commission of the Polish Academy of Arts and Sciences, Cracow, 7, 45–73, ISSN 1642-2511, 2005.

König, M., Nuth, C., Kohler, J., Mohold, G., and Pettersen, R.: A digital glacier database for Svalbard, in: Global Land Ice Measurements from Space, edited by: Kargel, J. S., Leonard, G. J., Bishop, M. P., Kääb, A., and Raup, B. H., Springer, Berlin, Heidelberg, Germany, 229–240, 2014.

Kosiba, A.: Some results of glaciological investigations in SW-Spitsbergen carried out during the Polish I.G.Y. Spitsbergen Expeditions in 1957, 1958 and 1959, Scientific Papers of University of Wrocław, B Series, 4, 30 pp., 1960.

Lefauconnier, B. and Hagen, J.O.: Surging and calving glaciers in eastern Svalbard, Norsk Polarinstitutt Meddelelser (Oslo), 116, 1–130, ISBN 82-9030794.2, 1991.

Lipert, C.: Prace geodezyjne w 50-leciu polskich wypraw polarnych, Sigma, Warszawa, Poland, 57 pp., 1962.

Luncke, B.: Luftkartlegningrn på Svalbard 1936, Norsk Geogr. Tidsskr., 6, 145–154, 1936.

Małecki, J.: Elevation and volume changes of seven Dickson Land glaciers. Svalbard, 1960–1990–2009, Polar Res., 32, 18400, https://doi.org/10.3402/polar.v32i0.18400, 2013.

Mannerfelt, E. S., Dehecq, A., Hugonnet, R., Hodel, E., Huss, M., Bauder, A., and Farinotti, D.: Halving of Swiss glacier volume since 1931 observed from terrestrial image photogrammetry, The Cryosphere, 16, 3249–3268, https://doi.org/10.5194/tc-16-3249-2022, 2022.

Marcinkiewicz, A.: Die zahlenmassige Erfassung des Gletscher-riickganges wàhrndder Periode 1936–1958 am zwei West-spitzbergen Gletschern, [in:] Bulletin de l'Académie Polonaise des Sciences, Série des Scienes Géologiques et Géographiques, 9, 233–237 + map, ISSN 0366-2497, 1961.

Martín-Moreno, R., Allende Álvarez, F., and Hagen, J. O.: "Little Ice Age'' glacier extent and subsequent retreat in Svalbard archipelago, Holocene, 27, 1–12, https://doi.org/10.1177/0959683617693904, 2017.

Maurer, J. and Rupper, S.: Tapping into the Hexagon spy imagery database: A new automated pipeline for geomorphic change detection, ISPRS J. Photogramm., 108, 113–127, https://doi.org/10.1016/j.isprsjprs.2015.06.008, 2015.

Maurer, J. M., Schaefer, J. M., Rupper, S., and Corley, A.: Acceleration of ice loss across the Himalayas over the past 40 years, Sci. Adv. 5, eaav7266, https://doi.org/10.1126/sciadv.aav7266, 2019.

McNabb, R., Nuth, C., Kääb, A., and Girod, L.: Sensitivity of glacier volume change estimation to DEM void interpolation, The Cryosphere, 13, 895–910, https://doi.org/10.5194/tc-13-895-2019, 2019.

Mertes, J. R., Gulley, J. D., Benn, D. I., Thompson, S. S., and Nicholson, L. I.: Using structure-from-motion to create glacier DEMs and orthoimagery from historical terrestrial and oblique aerial imagery, Earth Surf. Proc. Land., 42, 2350–2364, https://doi.org/10.1002/esp.4188, 2017.

Midgley, N. G. and Tonkin, T. N.: Reconstruction of former glacier surface topography from archive oblique aerial images, Geomorphology, 282, 18–26, https://doi.org/10.1016/j.geomorph.2017.01.008, 2017.

Morris, A., Moholdt, G., and Gray, L.: Spread of Svalbard Glacier Mass Loss to Barents Sea Margins Revealed by CryoSat-2, J. Geophys. Res.-Earth, 125, e2019JF005357, https://doi.org/10.1029/2019JF005357, 2020.

Nathorst, A. G.: Swedish explorations in Spitzbergen 1758–1908, Ymer (Stockholm), Sweden, 29 pp., 1909.

Noël, B., Jakobs, C. L., van Pelt, W. J. J., Lhermitte, S., Wouters, B., Kohler, J., Hagen, J. O., Luks, B., Reijmer, C. H., van de Berg, W. J., and van den Broeke, M. R.: Low elevation of Svalbard glaciers drives high mass loss variability, Nat. Commun., 11, 4597, https://doi.org/10.1038/s41467-020-18356-1, 2020.

Noormets, R. Flink, A., and Kirchner, N.: Glacial dynamics and deglaciation history of Hambergbukta reconstructed from submarine landforms and sediment cores, SE Spitsbergen, Svalbard, Boreas, 50, 29–50, https://doi.org/10.1111/bor.12488, 2020.

Nordli, Ø., Przybylak, R., Ogilvie, A., and Isaksen, K.: Long-term temperature trends and variability on Spitsbergen: The extended Svalbard Airport temperature series, 1898–2012, Polar Res., 33, 21349, https://doi.org/10.3402/polar.v33.21349, 2014.

Nordli, Ø., Wyszyński P., Gjelten H. M., Isaksen K., Łupikasza E., Niedźwiedź T., and Przybylak R.: Revisiting the extended Svalbard Airport monthly temperature series, and the compiled corresponding daily series 1898–2018, Polar Res., 39, 3614, https://doi.org/10.33265/polar.v39.3614, 2020.

Norwegian Polar Institute: Topografisk kart over Svalbard 1:100 000, C13. Sørkapp, Oslo, Norsk Polarinstitutt, 1948.

Norwegian Polar Institute: Topographic map of Svalbard 1:100 000, C13. Sørkapp, Oslo, Norsk Polarinstitutt, 1986.

Norwegian Polar Institute: Topographic map of Svalbard 1:100 000, C13. Sørkapp Land, Oslo, Norsk Polarinstitutt, 2007.

Norwegian Polar Institute: Terrengmodell Svalbard (S0 Terrengmodell) [data set], Norsk Polarinstitutt, https://doi.org/10.21334/npolar.2014.dce53a47, 2014.

Norwegian Polar Institute: Map archive [data set], Norwegian Polar Institute, https://doi.org/10.21334/npolar.2015.cf9a9474, 2015.

Nuth, C. and Kääb, A.: Co-registration and bias corrections of satellite elevation data sets for quantifying glacier thickness change, The Cryosphere, 5, 271–290, https://doi.org/10.5194/tc-5-271-2011, 2011.

Nuth, C., Kohler, J., Aas, H. F., Brandt, O., and Hagen, J. O.: Glacier geometry and elevation changes on Svalbard (1936–90): a baseline dataset, Ann. Glaciol., 46, 106–116, https://doi.org/10.3189/172756407782871440, 2007.

Nuth, C., Kohler, J., König, M., von Deschwanden, A., Hagen, J. O., Kääb, A., Moholdt, G., and Pettersson, R.: Decadal changes from a multi-temporal glacier inventory of Svalbard, The Cryosphere, 7, 1603–1621, https://doi.org/10.5194/tc-7-1603-2013, 2013.

Nuth, C., Moholdt, G., Kohler, J., Hagen, J. O., and Kääb, A.: Svalbard glacier elevation changes and contribution to sea level rise, J. Geophys. Res., 115, F01008, https://doi.org/10.1029/2008JF001223, 2010.

Oerlemans, J.: A flowline model for Nigardsbreen, Norway: projection of future glacier length based on dynamic calibration with the historic record, Ann. Glaciol., 24, 382–389, https://doi.org/10.3189/S0260305500012489, 1997.

Ostaficzuk, S., Lindner, L., and Marks, L.: Photogeological map of the Bungebreen forefield (West Spitsbergen), scale 1:10000, State Enterprise of Cartographic Publishing, Warszawa, 1982.

Osuch M. and Wawrzyniak T.: Inter- and intra-annual changes in air temperature and precipitation in western Spitsbergen, Int. J. Climatol., 37, 3082–3097, https://doi.org/10.1002/joc.4901, 2017.

Pälli, A., Moore, J., Jania, J. A., and Głowacki, P.: Glacier changes in southern Spitsbergen, Svalbard, 1901–2000, Ann. Glaciol., 37, 219–225, https://doi.org/10.3189/172756403781815573, 2003.

Pillewizer, W.: Die kartographischen und gletscherkundlichen Ergebnisse der Deutschen Spitzbergen Expedition 1938, Petermanss Geographische Mitteilungen Erganzh., Gotha, Germany, 238 pp., 1939.

Schöner, M. and Schöner, W.: Photogrammetrische und glaziologische Untersuchungen am Gåsbre (Ergebnisse der Spitzbergenexpedition 1991), Geowissenschaftliche Mitteilungen, Schriftenreihe der Studienrichtung Vermessungswesen der Technischen Universität Wien, Austria, 42, 120 pp. + 2 maps, ISSN 1811-8380, 1996.

Schöner, M. and Schöner, W.: Effects of glacier retreat on the outburst of Goësvatnet, southwest Spitsbergen, Svalbard, J. Glaciol., 43, 276–282, https://doi.org/10.3189/S0022143000003221, 1997.

Schuler, T. V., Kohler, J., Elagina, N., Hagen, J. O. M., Hodson, A. J., Jania, J. A., Käbb, A. M., Luks, Bartlomiej, Malecki, J., Moholdt, G., Pohjola, V. A., Sobota, I., and Van Pelt, W. J. J.: Reconciling Svalbard glacier mass balance, Front. Earth Sci., 8, 156, https://doi.org/10.3389/feart.2020.00156, 2020.

Sharov, A. I.: Exegesis of interferometric and altimetric observations in South Spitsbergen, The mass budget of Arctic Glaciers, edited by: Oerlemans, H., 88–93, Utrecht: IASC, IMAU, 2006.

Sharov, A. I. and Osokin, S. A.: Controlled interferometric models of glacier changes in south Svalbard, Proceedings of the Fringe 2005 Workshop, Frascati, Italy, 28 November–2 December 2005 (ESA SP-610), 1–8, 2006.

Stocker-Waldhuber, M., Fischer, A., Helfricht, K., and Kuhn, M.: Long-term records of glacier surface velocities in the Ötztal Alps (Austria), Earth Syst. Sci. Data, 11, 705–715, https://doi.org/10.5194/essd-11-705-2019, 2019.

Sund, M., Eiken, T., Hagen, J. O., and Kääb, A.: Svalbard surge dynamics derived from geometric changes, Ann. Glaciol., 50, 50–60, https://doi.org/10.3189/172756409789624265, 2009.

Surazakov, A. B. and Aizen, V. B.: Estimating volume change of mountain glaciers using SRTM and map-based topographic data, IEEE T. Geosci. Remote, 44, 2991–2995, https://doi.org/10.1109/TGRS.2006.875357, 2006.

Szafraniec, J.: Deglaciation rate on southern and western Spitsbergen in the conditions of Arctic amplification, Pol. Polar Res., 39, 77–98, https://doi.org/10.24425/118739, 2018.

Szafraniec, J.: Ice-Cliff Morphometry in Identifying the Surge Phenomenon of Tidewater Glaciers (Spitsbergen, Svalbard), Geosciences, 10, 328, https://doi.org/10.3390/geosciences10090328, 2020.

Teng, J., Wang, F., and Liu, Y.: An Efficient Algorithm for Raster-to-Vector Data Conversion, Geogr. Inform. Sci., 14, 54–62, https://doi.org/10.1080/10824000809480639, 2008.

Tielidze, L. G.: Glacier change over the last century, Caucasus Mountains, Georgia, observed from old topographical maps, Landsat and ASTER satellite imagery, The Cryosphere, 10, 713–725, https://doi.org/10.5194/tc-10-713-2016, 2016.

van Pelt, W., Pohjola, V., Pettersson, R., Marchenko, S., Kohler, J., Luks, B., Hagen, J. O., Schuler, T. V., Dunse, T., Noël, B., and Reijmer, C.: A long-term dataset of climatic mass balance, snow conditions, and runoff in Svalbard (1957–2018), The Cryosphere, 13, 2259–2280, https://doi.org/10.5194/tc-13-2259-2019, 2019.

Van Pelt, W. J. J., Schuler, T. V., Pohjola, V. A., and Pettersson, R.: Accelerating future mass loss of Svalbard glaciers from a multi-model ensemble, J. Glaciol., 67, 485–499, https://doi.org/10.1017/jog.2021.2, 2021.

Weber, P., Andreassen, L. M., Boston, C. M., Lovell, H., and Kvarteig, S.: An 1899 glacier inventory for Nordland, northern Norway, produced from historical maps, J. Glaciol., 66, 259–277, https://doi.org/10.1017/jog.2020.3, 2020.

WGMS: Global Glacier Change Bulletin No. 3 (2016–2017), edited by: Zemp, M., Gärtner-Roer, I., Nussbaumer, S. U., Bannwart, J., Rastner, P., Paul, F., and Hoelzle, M., ISC(WDS)/IUGG(IACS)/UNEP/UNESCO/WMO, World Glacier Monitoring Service, Zurich, Switzerland, 274 pp., https://doi.org/10.5904/wgms-fog-2019-12, 2020.

Zagrajski, S. and Zawadzki, A.: Polska Wyprawa na Spitsbergen 1934, Prace geodezyjne i kartograficzne, Military Geographical Institute, Library of the Topographic Service, Warsaw, 16, 102 pp. + 2 maps 1:50 000, 1936.

Zekollari, H., Huss, M., and Farinotti, D.: On the Imbalance and Response Time of Glaciers in the European Alps, Geophys. Res. Lett., 47, e2019GL085578, https://doi.org/10.1029/2019GL085578, 2020

Ziaja, W.: Glacial Recession in Sørkappland and Central Nordenskiöldland, Spitsbergen, Svalbard, during the 20th century, Arct. Antarct. Alp. Res., 33, 36–41, https://doi.org/10.1080/15230430.2001.12003402, 2001.

Ziaja, W.: Spitsbergen Landscape under 20th Century Climate Change: Sørkapp Land, Ambio, 33, 295–299, https://doi.org/10.1579/0044-7447-33.6.295, 2004.

Ziaja, W., Maciejowski, W., Ostafin, K.: Northeastern Sørkappland landscape dynamics (Spitsbergen, Svalbard), Jagiellonian University Press, Cracow, Poland, ISBN 978-83-233-2317-4, 2007.

Ziaja, W., Maciejowski, W., and Ostafin, K.: Coastal Landscape Dynamics in NE Sørkapp Land (SE Spitsbergen), 1900–2005, Ambio, 38, 201–208, https://doi.org/10.1579/0044-7447-38.4.201, 2009.

Ziaja, W. and Dudek, J.: Glacial recession, in: Transformation of the natural environment in Western Sørkapp Land (Spitsbergen) since the 1980s, edited by: Ziaja W., Jagiellonian University Press, Cracow, Poland, 51–60, ISBN 978-83-233-3231-2, 2011.

Ziaja, W. and Ostafin, K.: Landscape-seascape dynamics in the isthmus between Sørkapp Land and the rest of Spitsbergen: Will a new big Arctic island form?, Ambio, 44, 332–342, https://doi.org/10.1007/s13280-014-0572-1, 2015.

Ziaja, W., Dudek, J., and Ostafin, K.: Landscape transformation under the Gåsbreen glacier recession since 1899, southwestern Spitsbergen, Pol. Polar Res., 37, 155–172, https://doi.org/10.1515/popore-2016-0010, 2016.

Żyszkowski, J.: Photogrammetric Surveys In the Hornsund Fiord Area Spitsbergen, carried out in 1973, Results of Investigations of the Polish Scientific Spitsbergen Expeditions, Acta Universitatis Wratislaviensis, 4, 289–298, 1982.